Technical Report EL-95-13
March 1995

US Army Corps of Engineers
Waterways Experiment Station

Imaging Smolt Behavior on an Extended-Length Submerged Bar Screen and an Extended-Length Submerged Traveling Screen at The Dalles Dam in 1993

by John Nestler, Robert Davidson

Prepared for U.S. Army Engineer District, Portland

Technical Report EL-95-13
March 1995

Imaging Smolt Behavior on an Extended-Length Submerged Bar Screen and an Extended-Length Submerged Traveling Screen at The Dalles Dam in 1993

by John Nestler, Robert Davidson

U.S. Army Corps of Engineers
Waterways Experiment Station
3909 Halls Ferry Road
Vicksburg, MS 39180-6199

Final report

Approved for public release; distribution is unlimited

Prepared for U.S. Army Engineer District, Portland
P.O. Box 2946
Portland, OR 97208-2946

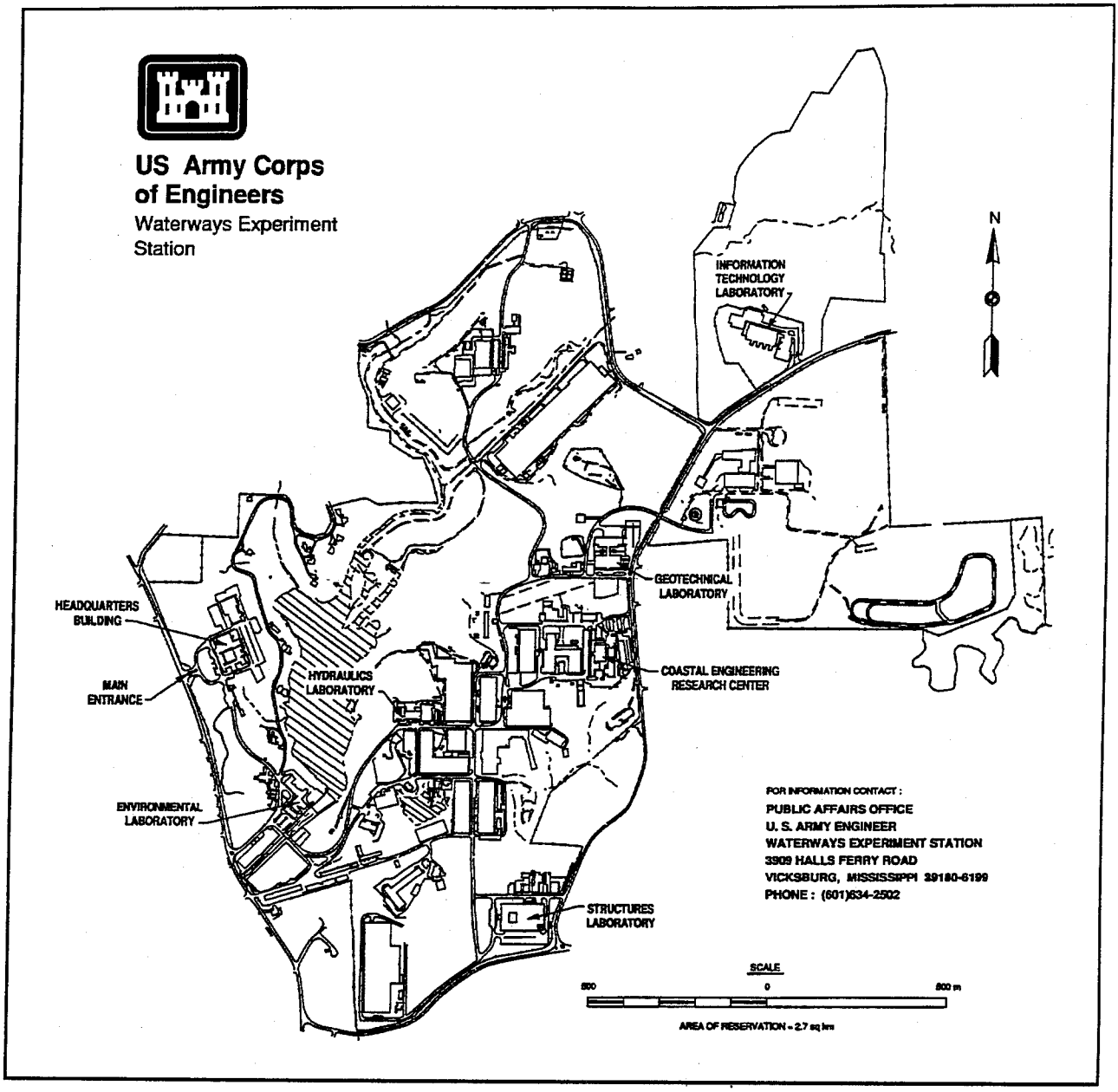

Waterways Experiment Station Cataloging-in-Publication Data

Nestler, John M.
Imaging smolt behavior on an extended-length submerged bar screen and an extended-length submerged traveling screen at the Dalles Dam in 1993 / by John Nestler, Robert Davidson ; prepared for U.S. Army Engineer District, Portland.
60 p. : ill. ; 28 cm. — (Technical report ; EL-95-13)
Includes bibliographic references.
1. Fish screens. 2. Underwater imaging systems. 3. Fishes — Behavior — Migration. 4. Dalles Dam (Or.) I. Davidson, Robert. II. United States. Army. Corps of Engineers. Portland District. III. U.S. Army Engineer Waterways Experiment Station. IV. Environmental Laboratory (U.S. Army Engineer Waterways Experiment Station) V. Title. VI. Series: Technical report (U.S. Army Engineer Waterways Experiment Station) ; EL-95-13.
TA7 W34 no.EL-95-13

Contents

List of Figures

List of Tables

Preface

This report compares impingement behavior of smolts on extended-length submerged traveling screens and extended-length submerged bar screens using underwater video imaging at The Dalles Dam during FY93. This report was prepared in the Environmental Laboratory (EL) and Hydraulics Laboratory (HL), U.S. Army Engineer Waterways Experiment Station (WES), Vicksburg, MS. The study was sponsored by the U.S. Army Engineer District, Portland, and was funded under Intra-Army order for Reimbursable Services No. E86930057 dated 18 February 1993.

The Principal Investigators of this study were Dr. John M. Nestler, Water Quality and Contaminant Modeling Branch (WQCMB), Environmental Processes and Effects Division, EL, and Mr. Robert Davidson, Locks and Conduits Branch, HL. This report was prepared by Dr. Nestler and Mr. Davidson under the direct supervision of Dr. Mark Dortch, Chief, WQCMB, and under the general supervision of Mr. Donald L. Robey, Chief, EPED, and Dr. John Harrison, Director, EL. This report was also prepared under the direct supervision of Mr. John George, Chief, Locks and Conduits Branch, and under the general supervision of Mr. Glenn Pickering, Chief, Hydraulic Structures Division, and Mr. Frank Herrmann, Director, HL. The assistance of Ms. Dottie Hamlin-Tillman, WQCMB, in the collation of data and editing of the report is gratefully acknowledged. Video imaging data were collected and processed by Messrs. Ahmed Darwish, contract student from Auburn University, Robert Jenkins, contract student from Jackson State University, and Jace Pugh, contract student from Millsaps College. Technical reviews by Messrs. Gene Ploskey and Tom Cole, WQCMB, and Ms. Hamlin-Tillman are gratefully acknowledged.

At the time of publication of this report, Director of WES was Dr. Robert W. Whalin. Commander of WES was COL Bruce K. Howard, EN.

This report should be cited as follows:

Nestler, John M., and Davidson, Robert A. (1995). "Imaging smolt behavior on an extended-length submerged bar screen and an extended-length traveling screen at The Dalles Dam in 1993," Technical Report EL-95-13, U.S. Army Engineer Waterways Experiment Station, Vicksburg, MS.

Conversion Factors, Non-SI to SI Units of Measurement

Non-SI units of measurement used in this report can be converted to SI units as follows:

Multiply	By	To Obtain
cubic feet per second	0.02831685	cubic meters per second
degrees (angle)	0.01745329	radians
feet	0.3048	meters
inches	0.0254	meters
miles (U.S. nautical)	1.852	kilometers

Executive Summary

During the spring of 1993, video imaging of smolt bypass systems at The Dalles Dam on the Columbia River was conducted using low-light sensitive underwater video cameras to contrast smolt behavior and impingement characteristics between an extended-length submerged traveling screen (ESTS) and an extended-length submerged bar screen (ESBS). Video images of the screen surface were obtained from six cameras located near the screen center line from the top (nearest the deck or intake) to the bottom of each screen. Cameras imaged laterally across the screen at locations 2, 13, 21, 26, 31, and 38 ft from the top of the ESBS and ESTS. The cameras on these bypass screens recorded smolt behavior to two porosities and three discharges. A total of 326 smolts grouped into 114 replicates were observed over a total duration of 11,760 min of imaging (imaging rate of approximately 0.03 smolts per minute). A total of 221 smolts separated into 42 replicates (each replicate having a minimum of 3 smolts) were used in the analysis of impingement characteristics of the two screen designs.

A variety of hydrodynamic and behavioral data were collected from each recorded image for the bypass screens. Data from physical model studies were used to supplement imaging data for some design or deployment configurations. Hydrodynamic data collected included direct measurements of water approach angle relative to the screen surface from the video images and variability in flow over time estimated using the standard deviation of multiple water angle measurements. Behavioral data collected included descriptions of the approach of the smolt to the screen (i.e., angle of approach, angle of retreat after a strike, orientation of the fish in the water) and descriptions of entrainment and impingement of smolts on the screen (e.g., entrainment without strike or impingement, strike with escape, impingement without escape, head-first approach without strike or impingement, and head-first approach with impingement).

Analysis of screen porosity was limited by inadequate numbers of replicates for the lower perforation plate porosity for each screen design. No conclusions could be reached on the effect of screen porosity. Impingement behavior variables differed by location on the screen. Screen impingement index and screen impingement tended to be highest at the middle camera location and passage without screen contact was lowest. Hydrodynamic conditions also varied by camera location. Flows were more nearly perpendicular

to the screen at its toe (nearest the trashrack) and more parallel to the screen at the top (nearest the draft tube deck). Screen design had a significant effect on a number of impingement behavior variables and the standard deviation of water approach angle. The ESTS consistently had lower impingement, reduced imaging rate, and increased standard deviation of water current angle.

We speculate that the more turbulent hydrodynamic conditions (as evidenced by the increased standard deviation of water approach angle) on the ESTS set up fluctuating pressure fields or velocity fields that the smolts can detect and hence more successfully avoid the traveling screens. In contrast, the bar screen is more hydrodynamically efficient and does not develop as extensive a fluctuating field and is, therefore, less detectable by smolts. The smolts are more likely to be imaged (because they are closer to the screen surface) and more likely to contact the bar screen than they are to be imaged on or contacted by the traveling screen.

1 Introduction

Background

The U.S. Army Corps of Engineers (USACE) operates hydropower dams on rivers that support valuable anadromous fisheries. Extensive bypass facilities have been installed at these dams to intercept out-migrating salmon smolts before they enter turbines. The first component of a bypass facility encountered by smolts is a submerged screen of relatively fine mesh or small bar spacing (the bypass screen). The bypass screen intercepts and guides smolts to the gatewell where another screen, the vertical barrier screen, guides smolts up the gatewell to a transport system that passes them around the dam and into the tailrace either for immediate release or for holding until later transport. Several screen designs and deployment configurations are being considered by the U.S. Army Engineer District, Portland (CENPP), to increase the efficiency of the bypass systems.

Studies at The Dalles Dam were based on studies conducted at McNary Dam in FY 91 and FY 92 using the most recent advances in underwater imaging systems to describe impingement behavior of smolts associated with alternative prototype screen designs (Nestler and Davidson 1993; Nestler and Davidson in preparation). Fish impingement is defined as the response of smolts to the presence of the screen which includes behaviors ranging from complete avoidance of the screen to impingement on the screen surface. Before these studies, real-time imaging of entrainment and impingement of smolts on prototype screens under operational conditions had rarely been performed. The success of McNary Dam studies suggested that videoimaging could be used at the Dalles to aid in the selection of screen design or deployment alternatives by CENPP.

Objectives

After mobilizing at The Dalles Dam, the U.S. Army Engineer Waterways Experiment Station (WES) staff was directed by CENPP to modify the study objectives as required in the contracted Scope of Work. The following revised objectives associated with fish passage efficiency and impingement were addressed.

a. Determine effects of localized water angle and water velocity on smolt impingement behavior.

b. Compare impingement characteristics of an extended-length submerged traveling screen (ESTS) to an extended-length submerged bar screen (ESBS).

c. Evaluate the effects of different perforation plate porosities. A perforation plate is a perforated plate that backs the screen. Flow pattern and water velocity through the screen can be controlled by the porosity of the perforation plate. Perforation plate porosities (referred to as screen porosities in the report) of 45 and 50 percent were evaluated for an ESBS. Porosities of 45 and 54 percent were evaluated for a ESTS.

d. Evaluate different unitloadings (11,000 through 15,000 cfs) on impingement behavior.

2 Materials and Methods

Site Description

The Dalles Dam is a multipurpose Corps of Engineers (CE) project located on the Columbia River at the head of Bonneville Lake at river mile 192.5 (Figure 1). It was authorized by the River and Harbor and Flood Control Act of May 1950 and presently consists (east to west) of: (a) two small house units to provide internal power requirements; (b) a powerhouse that accommodates 22 Kaplan turbines, two fishwater units, two station service units, a fish collection system, an assembly bay, and a control room; (c) spillway structure

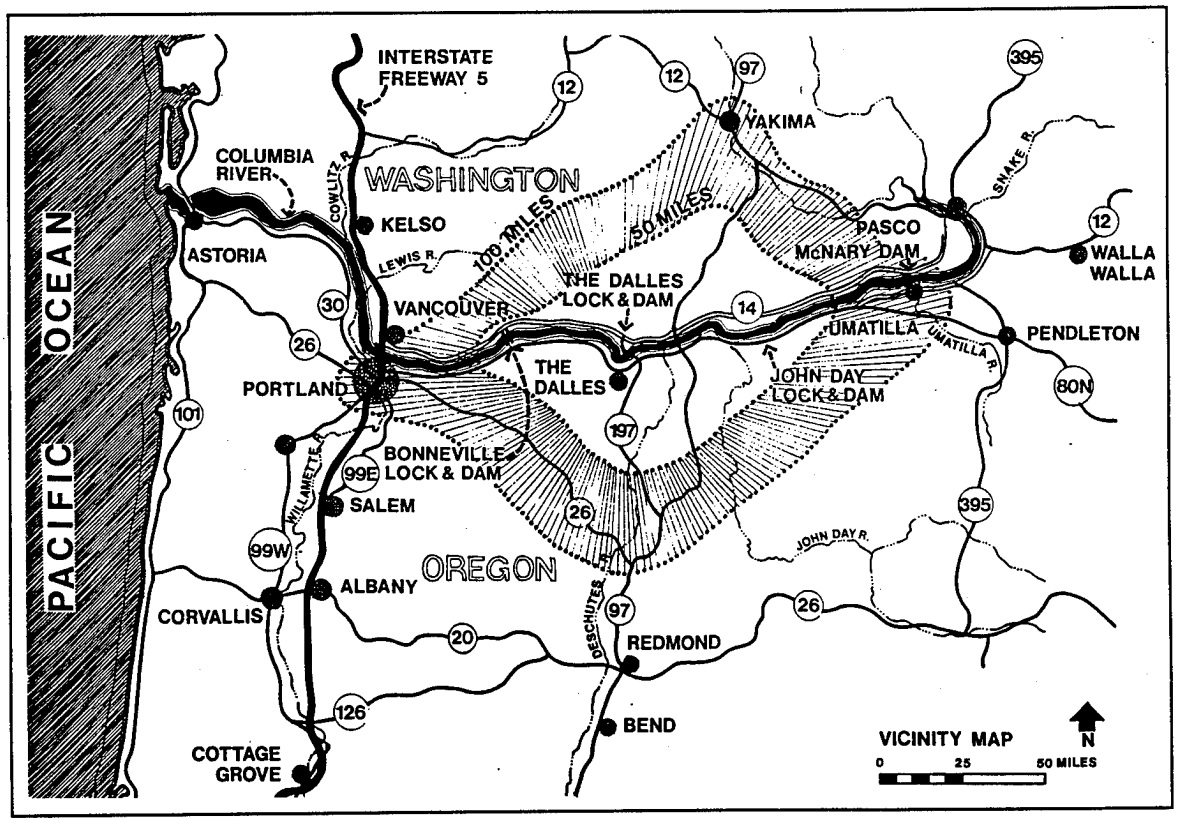

Figure 1. Site map showing location of The Dalles on the Columbia River

with 23 gates; (d) and a navigation lock (Figure 2). Power generation releases from the Dalles (Lake Celilo) are on a run-of-the-river basis and are closely governed by releases from the dams upstream and the flow requirements of the power projects downstream.

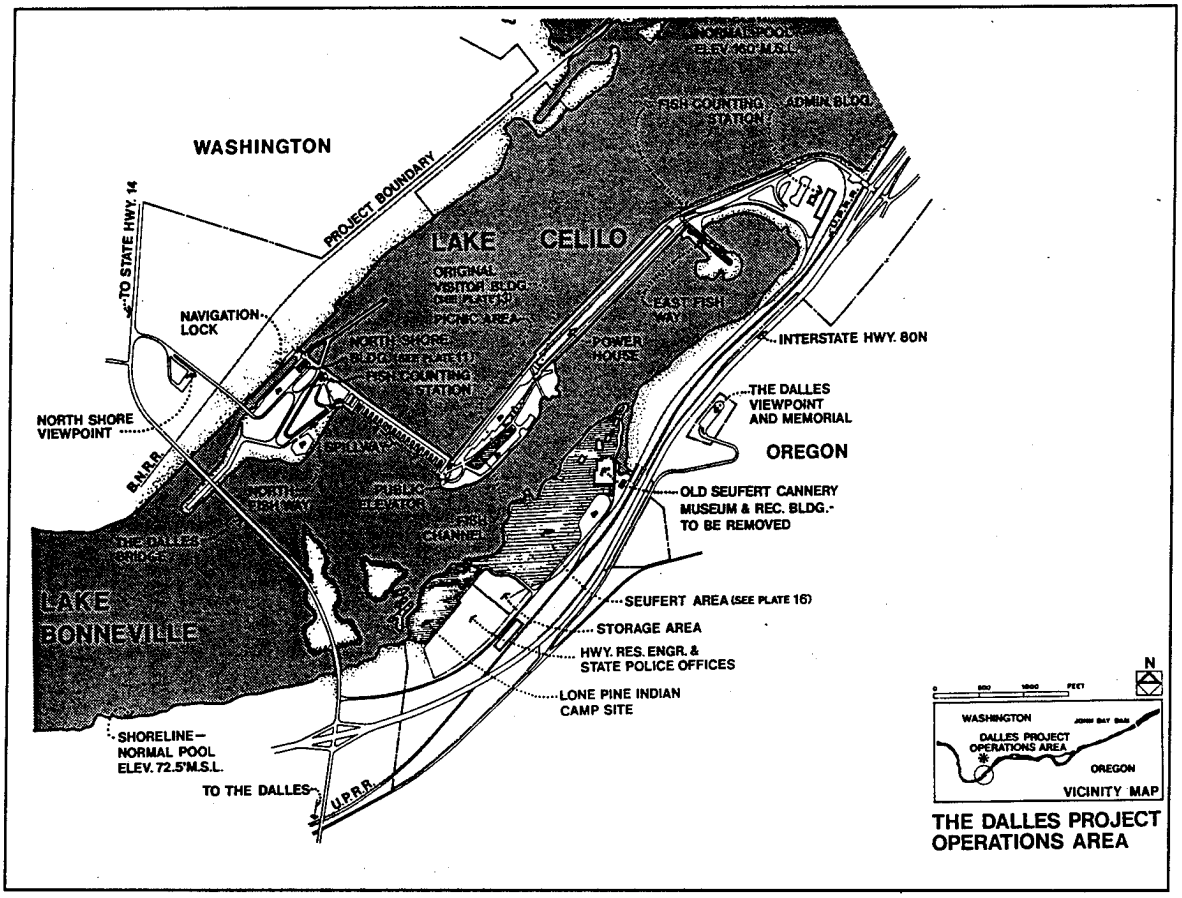

Figure 2. Plan view of The Dalles Dam showing approach channel and location of the powerhouse and spillway

The Dalles has extensive facilities to aid in the collection and transportation of both adult and juvenile migrating fishes. The primary structures of the fish passage system consist of the north fishway and fish ladder, the east fishway and fish ladder plus the interconnecting fish channel system, and the fish lock, which operates similar to the navigation lock but is used exclusively for fish migration. In recent years, bypass screens (i.e., extended submerged traveling and bar screens) have been installed to aid in guiding fish through the turbine penstocks (Figure 3). These screens divert the young fish away from the turbines and into a flume which carries them to a holding area where they await transportation downstream.

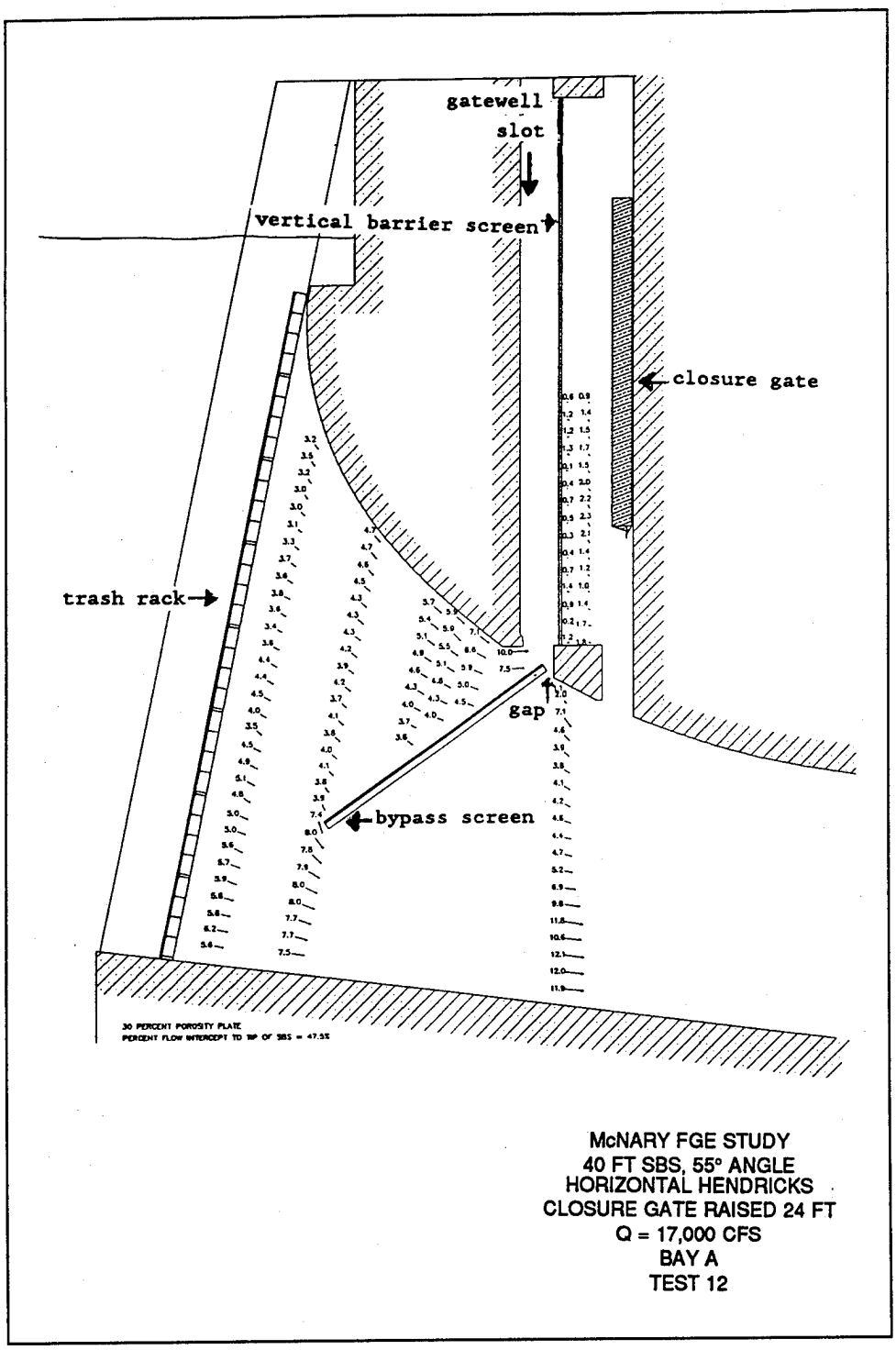

Figure 3. Profile view through a typical hydropower intake showing trashracks, an ESTS, a vertical barrier screen (VBS), and gatewell (slot in which VBS is stored). Velocity vectors were obtained from physical hydraulic model studies for this screen design and deployment configuration

Screen Descriptions

Two different bypass screen designs, an ESBS and an ESTS, were evaluated at the Dalles.

ESTS

The ESTS is the extended version of the standard screen utilized at CE dams on the Columbia River. The ESTS is 40 ft long and of sufficient width to completely span the width of the intake. The ESTS assembly consists of three frames: an outer support frame designed to slide in the gate slots for screen deployment and retrieval; an inner frame (attached to the outer frame) providing the structural support for the screen mesh; and an intermediate frame which connects the inner and outer frames and is used to set the deployment angle of the screen (Figure 4). The outer frame is made up of two support beams and two connecting tube beams. The inner frame is made up of two outer support beams, one center support beam, and several connecting box beams. Porosity plates span the space between the outer support beams of the inner frame. They are bolted from each outer support beam to the intermediate support beam. Porosity plates are used to control water velocity through the screen. Plates having different porosities can be used to manipulate water velocities through the screen. Nylon mesh screen is wrapped around the perimeter of the inner frame on each side of the center support beam to form two separate screen surfaces. The mesh from each screen surface extends from the center support beam to the outer support beam. The screens are rotated periodically to remove debris from the screen surface.

The inner frame is pinned to the outer frame at a pivot point near the top of the screen assembly, and the inner frame is supported by the intermediate frame deployed from the bottom of the screen assembly. The ESTS is deployed by lowering the screen assembly down a bulkhead slot in a collapsed (vertical) position. Once it reaches the desired elevation, the intermediate frame is extended which causes the inner frame to rotate about the pivot point. Deployment elevation can be varied, but usually the screen is deployed so that the top of the screen is 2.5 ft below the base of the Vertical Barrier Screen (MBFVBS) that concentrates and guides smolts up the gate slots. The intermediate frame is extended until the inner frame has been rotated to its desired operating angle, usually about 55 deg as measured from the vertical.

ESBS

The ESBS is one of two new screen designs that is being considered as a replacement for the standard-length submerged traveling screen (SSTS) on Columbia River Dams (Figure 5). The ESBS is 40 ft long and of a width

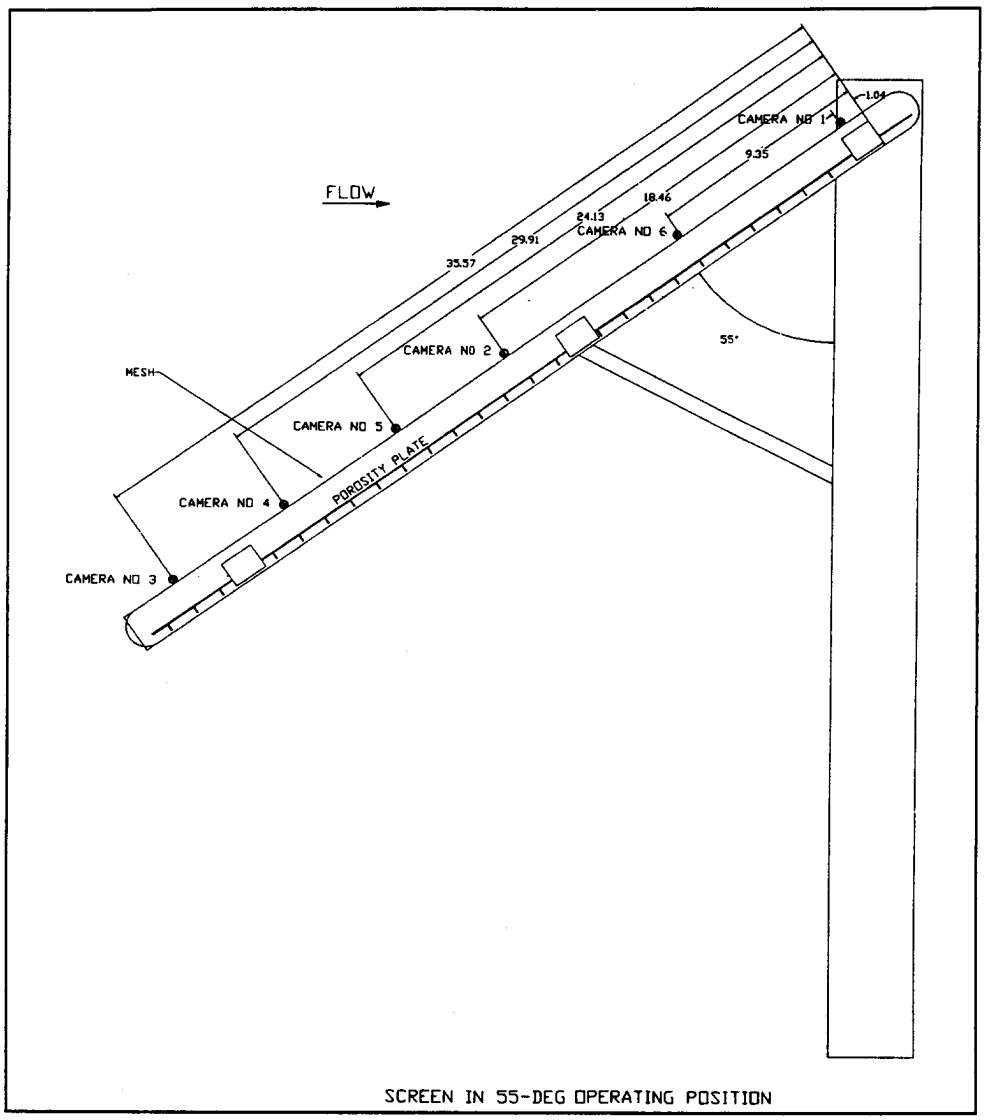

Figure 4. General configuration of an ESTS with approximate locations of video cameras indicated

sufficient to span the width of the intake. Like the ESTS, the ESBS assembly consists of three frames: an outer support frame designed to slide in the gate slot for screen deployment and retrieval; an inner frame made up of two outer support beams, two inner beams which support the tracks for the brush cleaning system, and a series of horizontal connecting box beams; an intermediate frame which connects the inner and outer frames and is used to set the deployment angle of the screen. Porosity plates span the space between the outer support beams of the inner frame. They are bolted from each outer support beam to the intermediate support beams. Porosity plates are used to control the velocity through the screen. The flat screen surface is comprised of 1/8-in. wedge wire with a 1/8-in. clear space running parallel to the center line of the screen reinforced on the underside at 6-in. intervals by U-bars.

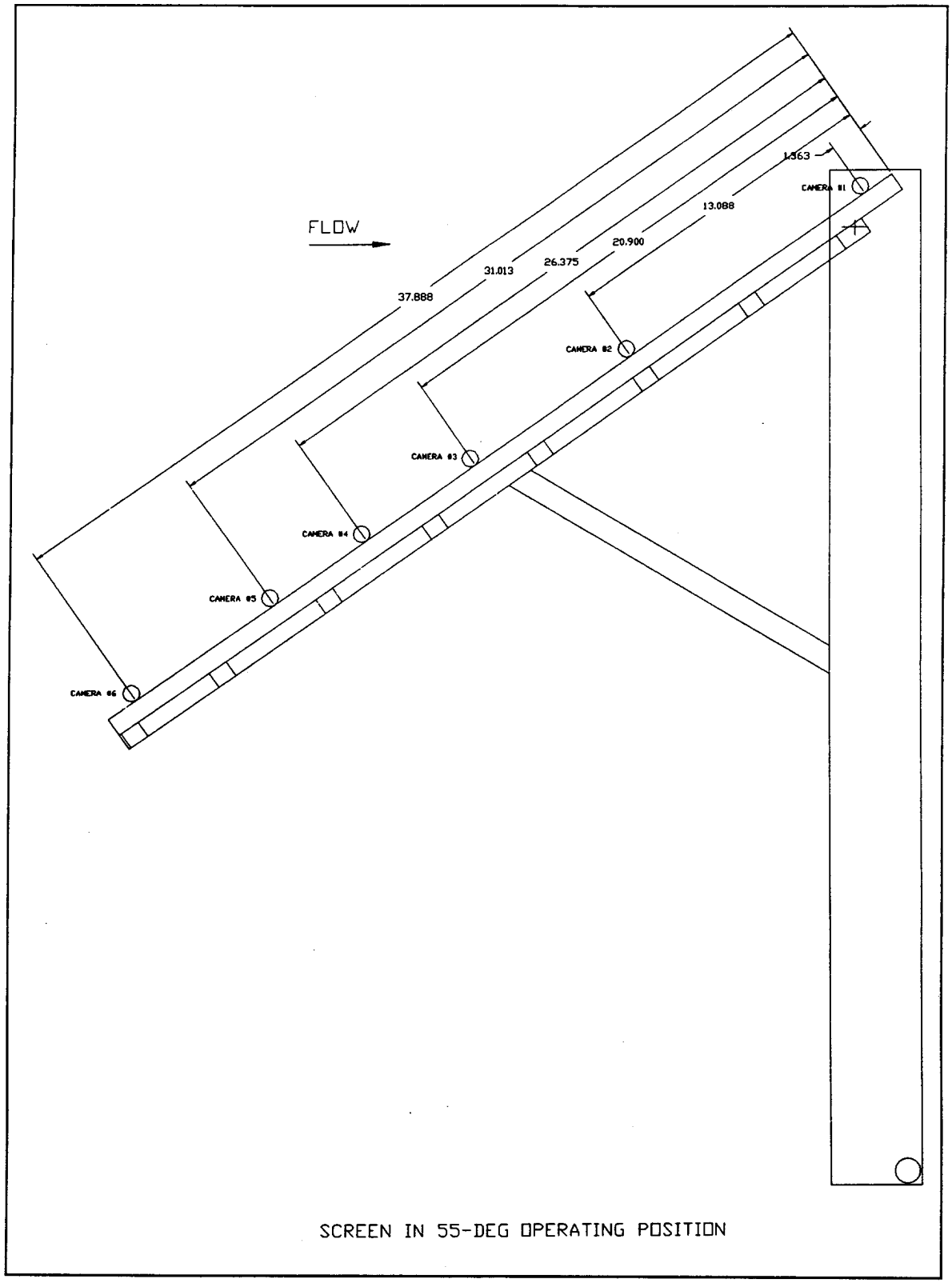

Figure 5. General configuration of an ESBS with approximate locations of video cameras indicated

The screen is supported by the perimeter of the inner frame on each side and the inner vertical members and the connecting horizontal box beams. The screen surface presented to the approaching flow is completely flat and uninterrupted by fasteners, tiedown bars, or other support members. The screen surface is swept by a automatic cleaning brush to prevent buildup of debris. The presence of the cameras prevented the automatic cleaning brush from being operated during imaging. The inner frame of the ESBS is pinned to the outer frame at a pivot point near the top of the screen assembly, and the inner frame is supported by the intermediate frames deployed from the bottom of the screen assembly. The ESBS is deployed and retrieved in a manner similar to the ESTS. The ESBS can have different porosity plates or alternative deployment configurations similar to the SSTS.

Camera and Illumination System

Three cameras were selected for use based on economics and availability. The first camera selected was the SL-99 Silicon-Intensified-Target (SIT) TV camera which is highly suited for conditions ranging from very low light to daylight conditions. Two less expensive cameras, the OE 1359 underwater solid state television camera and the DeepSea Power & Light Micro-SeaCam underwater video camera, were also used. Camera specifications for each type of camera are listed in Appendix A of Nestler and Davidson (in press).

Sampling Period and Conditions

FY 93 studies were performed between 1945 to 2400 hr at The Dalles Dam from 28 April to 25 May 1993 on days concurrent with fish guidance efficiency (FGE) testing conducted by the National Marine Fisheries Service (NMFS). In some cases, imaging occurred in bays used for FGE testing but at a time when NMFS staff had completed FGE testing. At other times, imaging occurred simultaneously to FGE testing but in units not used for FGE testing. Consequently, imaging performed in neighboring units should not be effected by the presence of the fyke net used during FGE testing. All tests were conducted without the fyke net, no closure gate, a 55-deg screen angle, and the screen at the normal elevation.

Bypass System Configuration

Intake configuration

The top of each bellmouth intake at The Dalles is located at elevation (el) 151.0,[1] a depth of 10.0 ft at normal pool. The bottom of the intake is located at el 58.0. Each intake is guarded by steel trashracks located approximately 21 ft upstream from the toe end of the ESBS and the ESTS.

Screen surface and gatewell

Findings by the WES Hydraulics Laboratory indicate that diversion screens generate complex hydrodynamic patterns that vary across the surface of the screen and change as screen design, angle, position, closure gate position, or unit loading is altered (e.g., compare hydrodynamic patterns in Figures 6 and 7. In addition, center, side, and cross supports of the screen produce local flow anomalies. The ability and propensity of fishes to respond to local flow conditions in rivers is well known. Not surprisingly, the complex hydrodynamic field on the screen surface results in localized differences in smolt behavior and impingement (Nestler and Davidson in press). Imaging was performed at multiple points to ensure that screen contact and impingement behavior of smolts is adequately quantified across the range of hydrodynamic conditions observed on the screen surface.

Imaging System Deployment

The camera mounting system used at The Dalles had to allow for normal deployment of the ESTS and ESBS through the gate slots and without a need for divers for attachment and inspection. The WES staff, with assistance from the Dalles project personnel, attached the light and camera system to the screen, secured cables, and performed other tasks necessary to complete attachment and installation of imaging equipment.

Camera mounting system

Cameras were inserted into a sleeve of 4.0-, 2.0-, or 1.58-in. inside diameter steel or aluminum pipe, as dictated by the diameter of the camera, and secured to the sleeve with set screws. The pipe was welded to a flat plate (Figure 8). The flat plate was bolted onto the nonmoving side support of the ESTS. For the ESBS, the flat plate was banded to the bar screen material

[1] Unless stated otherwise, all elevations (el) cited herein are in feet as referred to in the National Geodetic Vertical Datum (NGVD) of 1929.

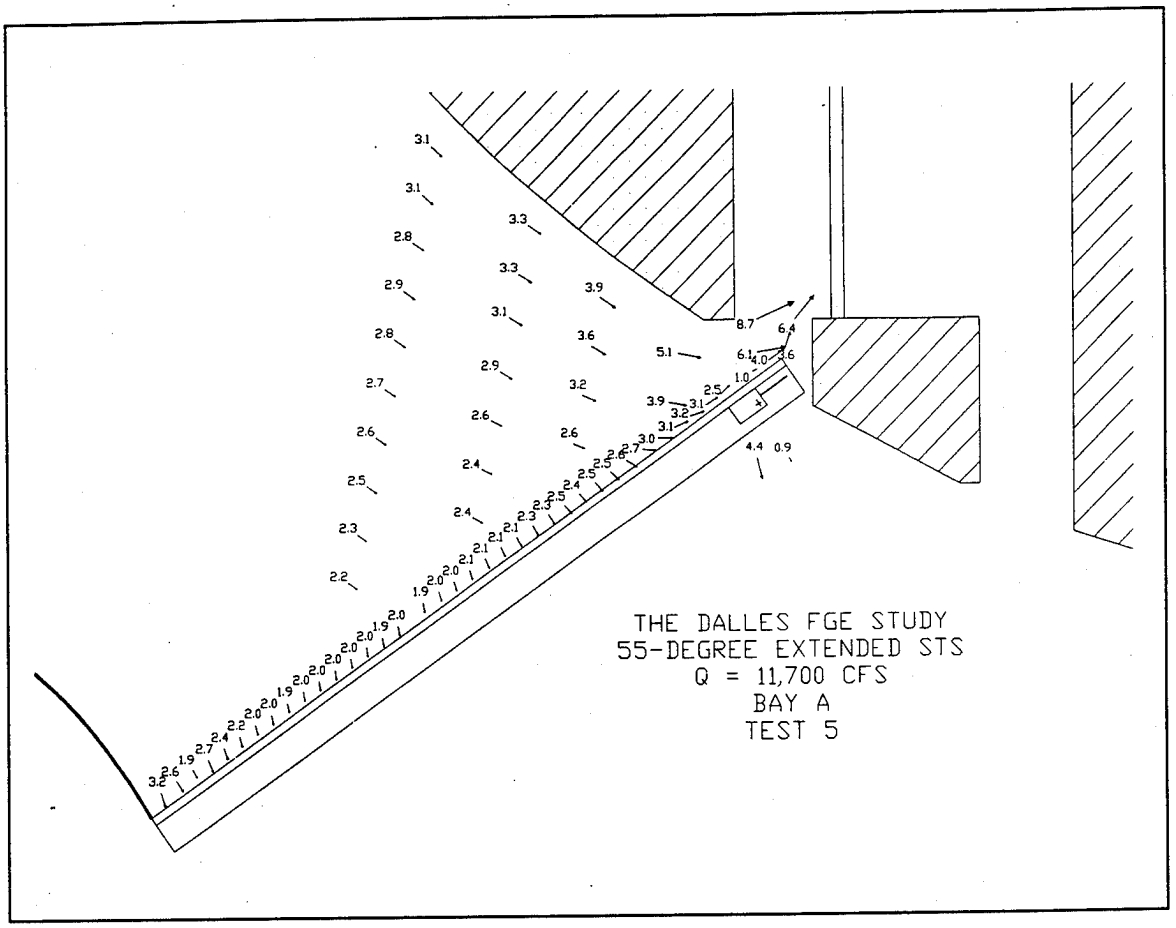

Figure 6. Side view of velocity distribution on surface of ESTS. Note how the direction and velocity of flow vectors change from toe to top of screen

using a stainless steel 0.5-in. banding material. Each camera on all screen types was aimed laterally across the surface of the screens. Camera depth-of-view, based on our ability to identify structural features (bolt heads on the tie down bar), was about 24 to 36 in. However, smolts are so highly reflective when illuminated from the side that they could be detected at distances estimated to be about 48 in.

Camera locations

Screen contact, impingement, and behavior of the smolts as they were intercepted by an ESTS or ESBS were imaged by six video cameras mounted along the sides of the different bypass screen types. Each camera imaged an area of the screen that had been previously identified through physical model studies as having hydrodynamic features that could affect impingement characteristics of smolts. Cameras imaged laterally across the screen at locations 2, 13, 21, 26, 31, and 38 ft from the top of the screen (Figures 4 and 5).

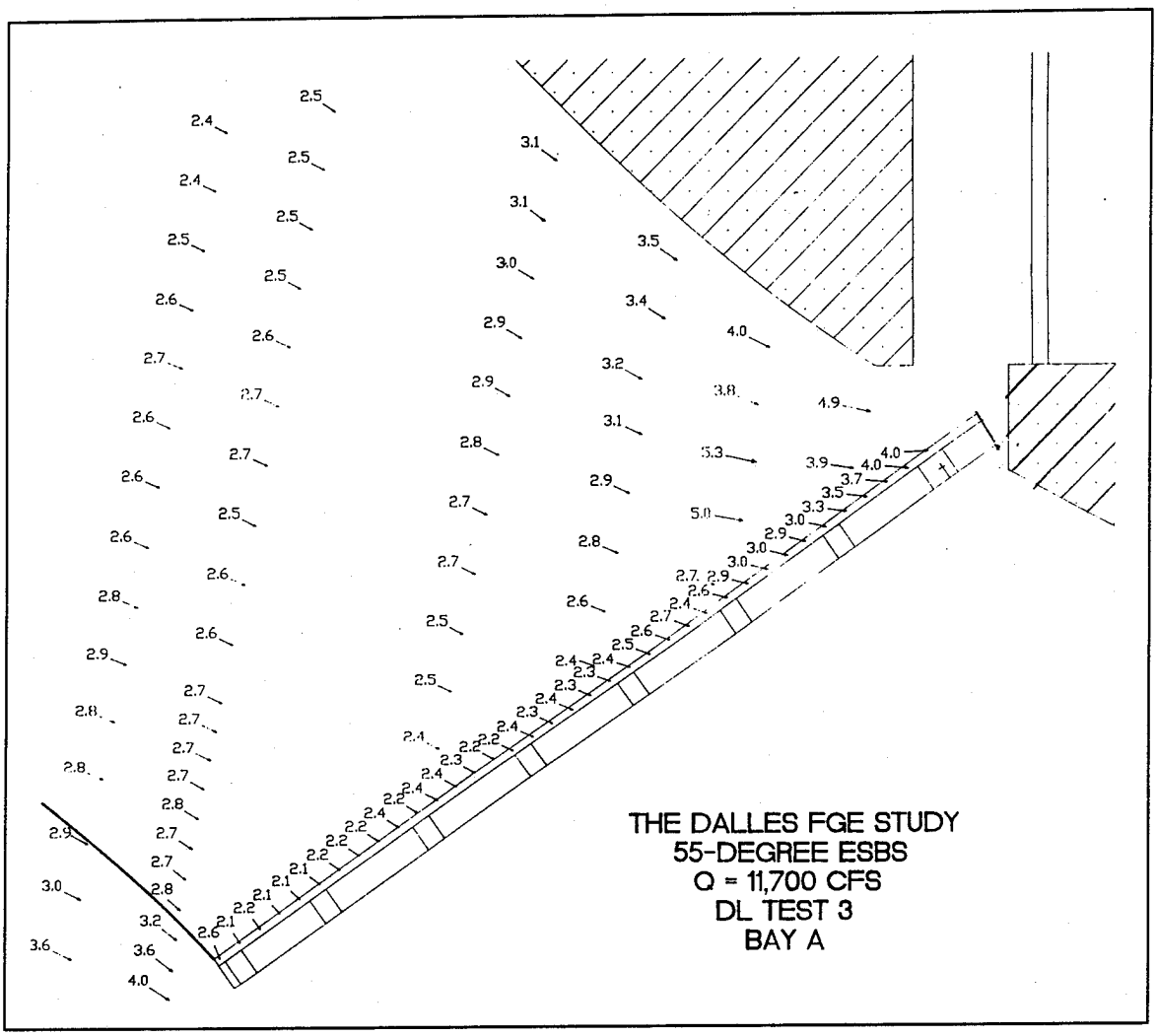

Figure 7. Side view of velocity distribution on surface of ESBS. Note how the direction and velocity of flow vectors change from toe to top of screen

In all cases the cameras on the bypass screen imaged from screen right to screen left. An incandescent light source with a maximum intensity of 250 watts was strapped to the pipe sleeve and aimed parallel to the aim of the camera or bolted to the flat plate and with the aim of the light directed parallel to the aim of the camera. Camera number 3 on the SSTS stopped operating shortly after the beginning of the study.

During imaging, each camera was connected to a video cassette recorder (VCR) and a television monitor. Field personnel observed each of the monitors and recorded the time that a smolt was observed on each tape in a log book that also contained screen design, deployment configuration, and related information. Usually two video cassettes were used nightly per camera with each cassette covering 2 hr of video imaging. Images were recorded on 180 video tapes with 80 documenting the ESBS and 100 documenting the ESTS. Each tape associated with bypass screens contained images of approximately 15 to 20 smolts, although some tapes recorded no events.

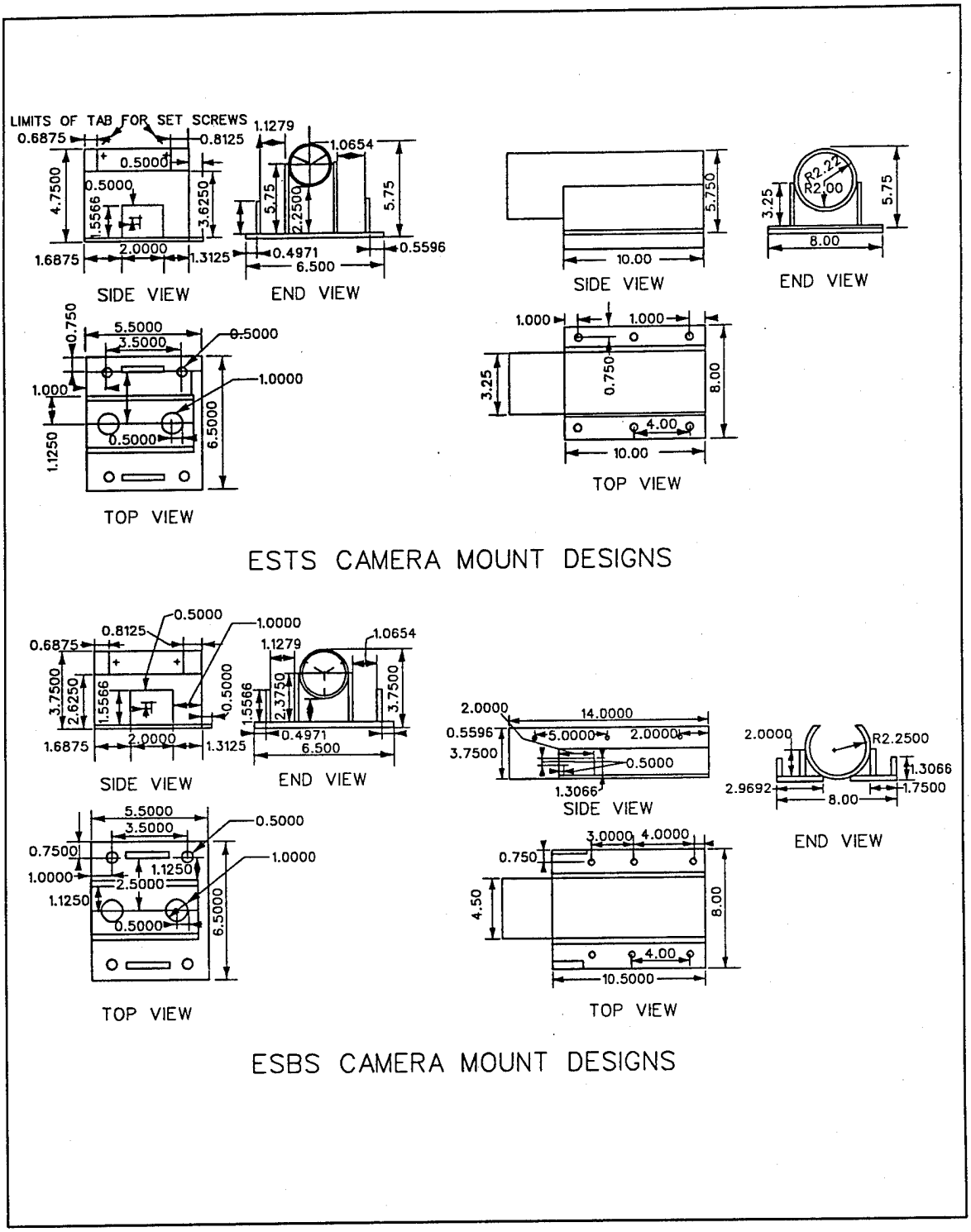

Figure 8. Camera mount designs used to image smolts on ESTS and ESBS

Imaging System Bias Evaluation

Describing impingement on and smolt behavior to bypass and vertical barrier screens using video imaging must address two potential experimental biases. First, the presence of the camera, illumination system, and mounting hardware will produce a significant hydrodynamic anomaly on an otherwise flat screen surface that may potentially influence fish response if the anomaly is large enough to be detected by and influence approaching smolts. Second, the illumination field required for camera imaging may also cause smolts to attract to or be repelled from the immediate vicinity of the camera and thus also bias any results describing fish response to bypass or vertical barrier screens. Studies to determine the significance of the bias introduced by the imaging study were conducted at McNary Dam in FY92 on an SSTS. The study and associated discussion indicated that neither the camera body or illumination system was having a detectable effect on the impingement behavior of smolts on an SSTS (Nestler and Davidson in press). Although we have no evidence to suggest that the highly reflective surface of an ESBS may provide enough reflection to affect fish behavior, we recommend that light bias be evaluated on a bar screen during future imaging work.

3 Data Analysis

Experimental Design

The cameras on the ESBS and ESTS recorded smolt behavior to two porosities per each screen design and a range of unitloads from 11 to 15 kcfs. For each deployment configuration, video imaging was used to collect multiple impingement events. The screen designs and deployment configuration evaluated are summarized in Table 1.

Table 1
Summary of Tests at The Dalles Dam in 1992. E = ESTS, X = ESBS

Screen	Test	Unit	Bay	Porosity	Angle	Elevation	Gate Pos	Fyke Net	Unit Loads, kcfs
ESBS/ ESTS	Screen Type	5 6	AB AB	45,50% 45,54%	55°	STD[1]	No Gate	A[2]	11, 12, 13, 15
ESBS/ ESTS	Unit Load	5 6	AB AB	45,50%	55°	STD	No Gate	A	11, 12, 13, 15
ESTS	Local Flow	6	A B	45%,54%	55°	STD	No Gate	A	11, 12, 13, 15
ESBS	Porosity	6	A	45%,50%	55°	STD	No Gate	A	12, 13, 15
ESTS	Porosity	6	A	45%,54%	55°	STD	No Gate	A	12, 13, 15
ESBS	Local Flow	6 7	A B	45%,50%	55°	STD	No Gate	A	12, 13, 15

[1] Standard position.
[2] Absent.

Smolt impingement characteristics associated with different screen designs or deployment configurations were evaluated by determining the proportion of smolts exhibiting different impingement responses during discrete blocks of time. Each of these time blocks was treated as a replicate. A minimum of three smolts had to be imaged during each replicate for that replicate to be included in the analysis of smolt impingement behavior. In some cases, when a particular condition was evaluated during a time period of reduced smolt passage, this relatively low number of smolts in a replicate will influence the

results. These situations are identified in the results section. Estimates of the angle of approach of the flow to the screen were based on replicates having as few as a single smolt. Variability in flow conditions (turbulence) on the screen surface was approximated by using the standard deviation of multiple water angle estimates obtained for each replicate.

Collection of Data from Video Tapes

Video camera images recorded on VHS format video tapes were played back on Panasonic monitors using a Sony VCR. Log-book entries made in the field were used to locate each image on the original video tapes. Each original video tape was reviewed and the fish-screen interaction was evaluated by a technician. The tapes were played back in slow motion and values for variables describing screen hydrodynamics and smolt passage, screen contact, impingement, and interception behavior (hereafter collectively termed impingement behavior) were recorded by a technician. Data encoding procedures and variable definitions for the bypass screens are presented in Appendix B of a report by Nestler and Davidson (in press).

Examples of smolt impingement events on an ESBS and on an SSTS are depicted in Figure 9.

Complex Variables

The data recorded by technicians describing smolt-screen interaction and the hydrodynamic environment were combined into complex variables, or indices, that could be used to describe and summarize the impingement characteristics of different screen designs and deployment configurations. The following variables and indices were employed to describe the impingement behavior of smolts on bypass screen. For each impingement or passage index except the impingement index, a smolt meeting the index requirement received a weighting of 1.0, whereas a smolt not meeting the index requirement received a weighting of 0.0. The impingement index added a "touch or strike with escape" category that received an intermediate weighting of 0.5. The 0.5 value was used because a "touch or strike" was assumed to be intermediate in its potential negative impact on the smolts between entrainment (without screen contact) and impingement. The force of the strike or touch was not considered.

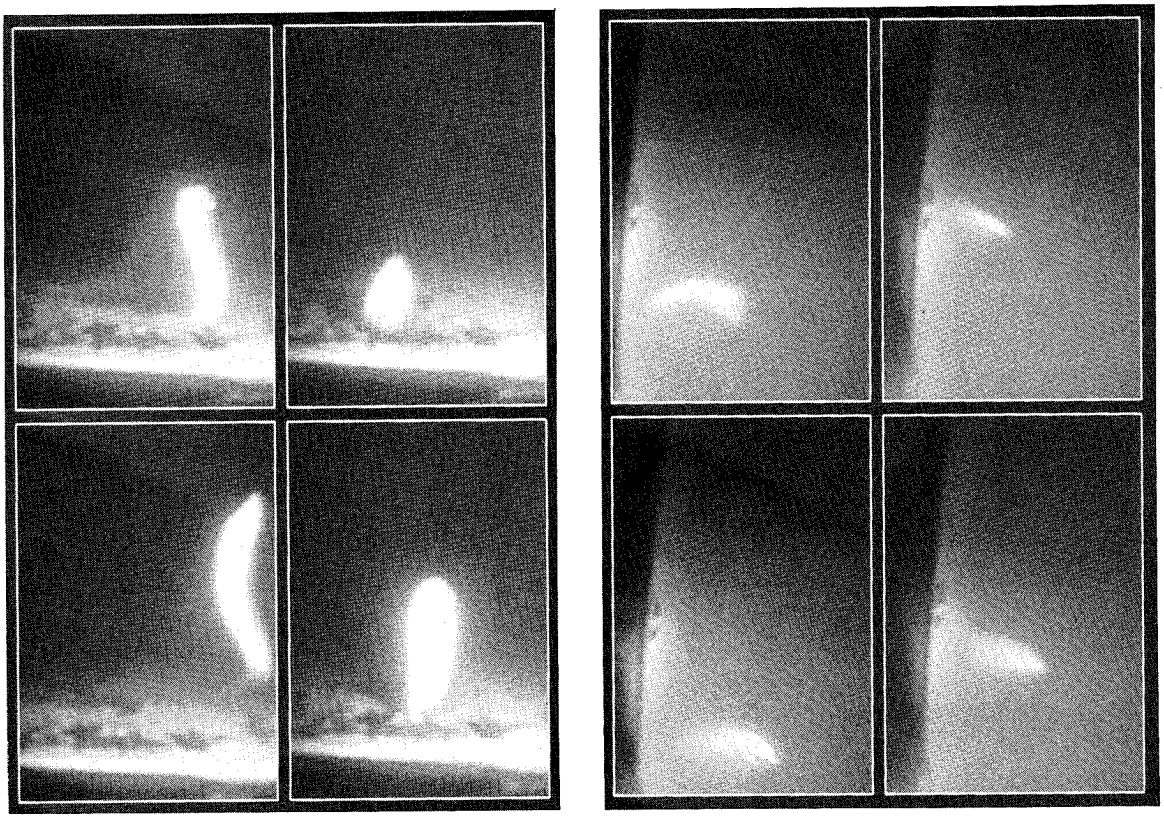

Figure 9. Examples of smolt impingement behavior on an ESBS (left block) and ESTS (right block). The mesh construction of the ESTS and the bar construction of the ESBS can be observed from the images. The angle of the image relative to the screen differs between the screen types. On both screens, the smolts are exhibiting contact with escape behavior. These interception events would both be entered into the data as "contact with escape"

a. R_PERMIN - Imaging Rate - The rate at which smolts are imaged as the number observed divided by the duration of imaging. This index can exhibit complex behavior because of its sensitivity to unitload. Increased unitload while smolt density (smolts/m^3) remains constant will result in an increase in the number of smolts moving through a fixed imaging field (imaging rate). In addition, increased unitload also increases water velocity through the screen so that smolts are more likely to be forced closer to the screen by the current and thus increase their probability of being imaged. Imaging rate should be evaluated with care because of its dependence on the complex effects and interactions of several independent variables.

b. R_IMPNEN - Entrainment Proportion - The number of smolts entrained that do not strike or touch the screen divided by the number of smolts observed.

c. R_IMPNES - Strike Proportion - The number of smolts that touch or strike the screen and escape divided by the number of smolts observed.

d. R_IMPNGD - Impingement Proportion - The number of smolts that impinge on the screen and do not escape divided by the number observed.

e. R_IMPNGI - Impingement Index - The number of smolts that either touch, strike, or impinge on the screen divided by the number observed (for this index a smolt that touches or strikes the screen but does not impinge receives a weighting of 0.5).

f. R_IMPNGN - Entrained Headfirst - The number of smolts entrained head-first that do not touch or strike or strike the screen. Although speculative, it seems reasonable that optimum guidance occurs when the smolt is moving headfirst parallel to the direction of flow without striking the screen. This orientation implies that the smolt is being guided efficiently and has not touched or stuck the screen. Smolts that strike the screen often reorient and move headfirst into the flow with its tail striking the surface of the screen.

g. R_IMPNGH - Headfirst Strike - The number of smolts that are entrained headfirst and are observed to touch or strike the screen and impinge.

h. CURR_ANG - Mean Current Angle 0° to 180° - Mean water current angle ranging from 0°-180° with 0° representing water flow moving parallel to the screen away from the gateslot and 180° representing water flow moving parallel to the screen surface towards the gate slot.

i. CUR_ANG9 - Mean Current Angle 0° to 90° - Mean water current angle ranging from 0° to 90° calculated as the absolute value of the current angle with 0° representing flow perpendicular to the screen and 90° representing water flow moving parallel to the screen in either direction.

j. CURR_CV - Variance in Current Angle - Variance in current angle over time used as a surrogate for turbulence. More turbulent flow conditions on the screen will produce a greater variance.

k. CRAN9_CV - Current Angle Plus Variance - The mean current angle plus the variance in mean current angle. This variable attempts to integrate both variation in flow and flow angle.

l. CR_ANGRD - Physical Model Current Angle - The mean current angle determined from physical hydraulic model studies rounded to nearest 10 deg.

m. CR_VELRD - Physical Model Current Velocity - The mean current velocity determined from physical hydraulic model studies rounded to nearest foot per second.

The above indices were selected not only because they characterize different entrainment behaviors but also because they vary in their data requirements. The Impingement Index provides only very general information but, in compensation, is not data intensive because a number of different impingement categories will produce an increase in this index. This index is most likely to provide useful information for those conditions where few smolts are available for analysis. The indices requiring more observations, such as the two "Headfirst Indices," can provide detailed information for those conditions having many images but are of limited usefulness when the passage rate of smolts is low, because relatively few smolts meet the requirements of this index. Consequently, the headfirst indices must be used with caution because their values may be determined by only one or two smolts. Two measures of current angle were used to ensure that the reference system for current angle did not unduly influence the analysis. Variance in current angle is used as a surrogate for turbulence.

Data Analysis

Data analysis for the bypass screens was performed using the Statistical Analysis System (SAS Institute 1988). Data analyses were performed at two levels.

First, general analyses were performed for the ESBS only to determine the effects of water velocity and water approach angle on the impingement variables defined earlier but without consideration of screen deployment configuration or camera location. Too few observations were available to perform the general analysis on the ESTS data. Second, detailed analyses were performed to determine the effects of specific screen design or deployment configurations on impingement variables.

Statistical power analysis (Peterman 1990) was considered but not performed. Statistical power analysis would provide information on the probability of rejecting a null hypothesis when it is false. However, the major data inadequacy occurs in the formation of proportions based on relatively few fishes. Statistical power analysis would not address this problem. In lieu of statistical power analysis, we have included the number of observations upon which the proportions are based for all summary tables so that those analyses based on relatively few observations can be readily identified.

Local hydrodynamic conditions

These general analyses were performed to determine the response of smolts to local hydrodynamic conditions at the point where they are intercepted by the screen without consideration of their location on the screen. Potentially, the results of the general analyses can be used to develop design guidelines or optimize deployment configurations. Separate analyses were performed for the two screen designs. For the ESBS, sufficient physical hydraulic model

data were available to use with the videoimaging data. For the ESTS, only data collected by videoimaging were available for analysis. The general analyses were comprised of the following four steps.

a. Summary tables were constructed providing means of variables for each screen design or deployment configuration. These tables provide expanded information that can be used to interpret results of the ANOVA.

b. Correlation analysis (PROC CORR) was used to determine general relationships among independent and dependent variables. In particular, relationships between independent variables were explored to determine possible confounding effects among independent variables. For some cases, either because of logistical restraints or dam operator convenience, application of the treatments was not random but occurred in a set pattern over time. The confounding effects of correlated independent variables must be considered in interpreting the results of the analysis. Correlation analysis was also used to examine patterns of response among the dependent variables. In cases where the number of smolts per replicate was limited or the number of replicates was limited, effects of a particular independent variable were inferred, based on observing a consistent pattern across several correlated dependent variables.

c. Analysis of variance (ANOVA) using the General Linear Models Procedure (PROC GLM of SAS) was used to test for the effects of different treatments on dependent variables describing smolt impingement behavior or hydrodynamic patterns on the bypass screen. Analyses were considered to be significant at $\alpha=0.05$. However, analyses significant at up to $\alpha=0.20$ (and highlighted by bolding) were evaluated, but considered only when they fell within consistent patterns across treatments or replicates. In many cases, we were hindered by small sample size and it seemed prudent to lessen the rigor of the criteria used to determine significance to reduce the probability of accepting a false null hypothesis. In all cases, we tested the null hypothesis that sample means were identical.

d. Regression analysis using backward elimination (PROC REG of SAS) was used to build statistical models to predict impingement behavior variables using hydrodynamic variables as independent variables. Backward elimination was employed so that quadratic effects could be evaluated. If successful, the regression equations could be used to infer the impingement characteristics across a screen surface if the hydrodynamic patterns across the screen could be determined either from physical hydraulic model studies or from video imaging analysis of prototype screens during time periods when smolts were not passing.

Detailed analyses

Detailed analyses were performed using ANOVA to determine the effects of different camera locations, unitloads, porosities, and screen designs on hydrodynamic conditions and impingement characteristics. Separate analyses were performed for each treatment in blocked designs because insufficient data were available to perform two-way or three-way ANOVA.

The detailed analyses were performed in two phases. In the first phase, the imaging results of all cameras combined were used to provide information on the overall impact of a particular screen design or deployment configuration on hydrodynamic variables and impingement characteristics.

In the second phase, analyses were performed using the imaging results for each camera separately allowing the effects of different deployment configurations to be related to specific positions on the screens. The experimental design is summarized in Table 1.

4 Results

General

This chapter contains results of statistical analyses for the bypass screen evaluations, and its organization generally follows Table 1, except where noted.

The bypass screen evaluation is separated into five sections. The first section presents summary statistics to describe general patterns between and among variables. The first section also includes correlation analysis of the dependent and independent variables. The second section describes the results of studies to determine the response of smolts to localized hydrodynamic conditions (immediate velocity and current angle) on the screen surface 13, 21, 26, 31, and 38 ft from the top of the screen. It includes summary tables, ANOVA to determine the effects of hydrodynamic variables on impingement behavior, and regression analysis to determine if local hydrodynamic variables can be used to predict impingement behavior. The third section presents tabular summaries and results from ANOVA for camera location. The fourth section evaluates the effects of unitload, the fifth for screen porosity, and the sixth section describes the effects of screen design on impingement behavior.

Summary Statistics

Summary tabulations

Table 2 presents summary data and simple statistics for the dependent and independent variables used in the analyses. Hydraulic data from physical model studies of the ESBS were available for some unitloads and screen porosities. It was possible to extrapolate both water velocity and water angle results from the model studies to the prototype screen. Physical model data, when available, were used in lieu of observed hydrodynamic data obtained from the video cameras. Note that the imaging rate (R_PERMIN) of 0.06 smolts/min for The Dalles was approximately equal to the imaging rate for spring time sampling at McNary Dam in 1992 of 0.08 smolts/min.

Table 2
Simple Statistics for Dependent and Independent Variables

Variable	N	Mean	Std Dev	Sum	Minimum	Maximum
R_PERMIN	42	0.060240	0.077630	2.599800	0.025000	0.520000
R_IMPNEN	42	0.510440	0.282508	21.438462	0	1.000000
R_IMPNES	42	0.278550	0.220554	11.699084	0	0.666667
R_IMPNGI	42	0.266152	0.166900	11.178388	0	0.666667
R_IMPNGD	42	0.046040	0.106163	1.933700	0	0.428571
R_IMPNGH	42	0.016270	0.064863	0.683333	0	0.333333
R_IMPNGN	42	0.025942	0.073175	1.089560	0	0.285714
R_SDEAD	42	0.005952	0.038576	0.250000	0	0.250000
SCRNPORE	42	51.238095	2.809475	2152.000000	45.000000	54.000000
HOURBEG	42	20.952381	1.010973	880.000000	20.000000	22.000000
UNITLOAD	42	13.428571	1.039298	564.000000	12.000000	15.000000
SCREEN	42	1.523810	0.505487	64.000000	1.000000	2.000000
CURR_ANG	42	127.380952	9.385906	5350.000000	100.000000	150.000000
CUR_ANG9	42	37.380952	9.385906	1570.000000	10.000000	60.000000
CUR_ANCV	42	34.523810	10.865560	1450.000000	10.000000	60.000000
CURR_CV	42	2.857143	4.572300	120.000000	0	10.000000

Note: Extended traveling screen = 1 = E; Extended bar screen = X = 2.

However, the impingement index of 0.266 and the impingement proportion of 0.046 (4.6 percent impinged) were less than one-half of the values for these same variables for the McNary Dam study (Nestler and Davidson in preparation), the only other study in which videoimaging was systematically employed to determine the impingement characteristics of different screen design or deployment alternatives. The biggest difference between The Dalles and McNary Dams is in the range of water approach angles to the screen. In general, the water current at The Dalles is much less variable (standard deviation of water angles is 9 deg for The Dalles Dam and 21 deg for McNary Dam) and more parallel to the slant of the bypass screen than the water current at McNary Dam (mean water current of 127 deg for The Dalles and 123 deg for McNary Dam.

Correlation analysis

Correlation analysis (Table 3) of the impingement/entrainment (dependent) variables indicated the following:

Table 3
Pearson Correlations for Dependent Variables

	R_PERMIN	R_IMPNEN	R_IMPNES	R_IMPNGI	R_IMPNGD	R_IMPNGH	R_IMPNGN	R_SDEAD	CURR_ANG	CURR_CV	CR_VELRD
R_PERMIN	1.00000 0.0	-0.04503 0.7770	-0.07397 0.6415	0.03739 0.8141	0.05690 0.7204	-0.07829 0.6221	0.24181 0.1229	-0.05478 0.7304	0.10127 0.5234	-0.09003 0.5707	0.05512 0.8280
R_IMPNEN	-0.04503 0.7770	1.00000 0.0	-0.54522 0.0002	-0.95408 0.0001	-0.31435 0.0426	-0.20989 0.1822	0.09138 0.5649	-0.28560 0.0667	0.19387 0.2186	0.02130 0.8935	0.21086 0.4010
R_IMPNES	-0.07397 0.6415	-0.54522 0.0002	1.00000 0.0	0.46086 0.0021	-0.03581 0.8219	-0.02853 0.8577	0.03796 0.8113	-0.02046 0.8977	0.10377 0.5131	0.07723 0.6269	-0.29640 0.2324
R_IMPNGI	0.03739 0.8141	-0.95408 0.0001	0.46086 0.0021	1.00000 0.0	0.58058 0.0001	0.34031 0.0274	-0.08390 0.5973	0.33986 0.0277	-0.27206 0.0813	-0.06005 0.7056	-0.05959 0.8143
R_IMPNGD	0.05690 0.7204	-0.31435 0.0426	-0.03581 0.8219	0.58058 0.0001	1.00000 0.0	0.53891 0.0002	-0.01333 0.9332	0.30368 0.0506	-0.33062 0.0325	-0.15199 0.3366	0.19370 0.4412
R_IMPNGH	-0.07829 0.6221	-0.20989 0.1822	-0.02853 0.8577	0.34031 0.0274	0.53891 0.0002	1.00000 0.0	-0.09110 0.5661	0.56959 0.0001	-0.22877 0.1450	-0.16057 0.3097	
R_IMPNGN	0.24181 0.1229	0.09138 0.5649	0.03796 0.8113	-0.08390 0.5973	-0.01333 0.9332	-0.09110 0.5661	1.00000 0.0	-0.05604 0.7245	0.13685 0.3875	0.12714 0.4223	-0.50082 0.0343
R_SDEAD	-0.05478 0.7304	-0.28560 0.0667	-0.02046 0.8977	0.33986 0.0277	0.30368 0.0506	0.56959 0.0001	-0.05604 0.7245	1.00000 0.0	-0.46112 0.0021	-0.09877 0.5337	0.00000 1.0000
CURR_ANG	0.10127 0.5234	0.19387 0.2186	0.10377 0.5131	-0.27206 0.0813	-0.33062 0.0325	-0.22877 0.1450	0.13685 0.3875	-0.46112 0.0021	1.00000 0.0	-0.10555 0.5059	0.31633 0.2009
CURR_CV	-0.09003 0.5707	0.02130 0.8935	0.07723 0.6269	-0.06005 0.7056	-0.15199 0.3366	-0.16057 0.3097	0.12714 0.4223	-0.09877 0.5337	-0.10555 0.5059	1.00000 0.0	0.56980 0.0136
CR_VELRD	0.05512 0.8280	0.21086 0.4010	-0.29640 0.2324	-0.05959 0.8143	0.19370 0.4412		-0.50082 0.0343	0.00000 1.0000	0.31633 0.2009	0.56980 0.0136	1.00000 0.0

Note: All instances in which three or more smolts were observed, except for the CR_VELRD (water velocity at screem surface as predicted from physical hydraulic models) which was based on one observation. All correlation coefficients are based on N = 42, except for CR_VELRD which is based on N = 18.

a. The passage index (no impingement or screen contact - R_IMPNEN) was negatively correlated to the impingement variables (impingement or screen contact - R_IMPNGI, R_IMPNGD, R_IMPNES). There was no significant correlation between the headfirst passage index (R_IMPNGN) and the impingement variables.

b. Increasing current velocity (CR_VELRD) did not affect the impingement variables (R_IMPNGD and R_IMPNGI) or passage indices except headfirst entrainment without impingement (R_IMPNGN) which was negatively correlated to increasing water velocity.

c. Increasing water angle decreases the impingement index ($P=0.0813$), decreases impingement proportion (at $P=0.0325$), and increases the passage indices, although the rates for the passage indices are not significant at $\alpha=0.2000$.

d. Current angle and velocity are positively correlated, although this is probably an artifact of the analysis because the upper camera locations where the flow is more parallel to the screen is underrepresented in the data set.

e. The effects of changing current angle appear to exceed (has higher correlation coefficients and more significant probabilities) the effects of changing water velocity over the range of values available for this analysis.

f. R_IMPNGI and R_IMPNGD are correlated ($r=0.58$, $P=0.0001$), suggesting that when observations are sparse R_IMPNGI (which has reduced data requirements) is a good surrogate for R_IMPNGD.

g. Water velocity and (CR_VELRD) and turbulence (CURR_CV) were highly correlated ($r=0.57$, $P=0.0136$), suggesting that increasing water velocity sets up hydrodynamic instabilities on the screen.

The results of correlation analysis of independent variables for the spring is found in Table 4. The hydrodynamic variables are included in both the dependent and independent correlation analyses. There were a number of highly significant correlation coefficients ($p < 0.01$) among the independent variables, but none of the correlation coefficients were greater than 0.44, (e.g., the correlation coefficient between unitload and perforation plate porosity of 0.42 means that 0.18 (0.42^2) percent of the variance in one variable is explained by the other), and few were greater than 0.20, suggesting that, generally, confounding effects were minimal. Of greatest interest, unitload, screen design, and screen porosity were not randomized. That is, the same unitloads and screen porosities were not employed for each of the two screen designs. Also, standard deviation of water angle, a surrogate for turbulence was highly affected by both screen design and screen porosity ($P<0.01$).

Table 4
Pearson Correlations of Independent Variables Using all Replicates in Which One or More Smolts Were Observed

	SCREEN	SCRNPORE	HOURBEG	UNITLOAD	R_PERMIN	CURR_ANG	CUR_ANG9	CUR_ANCV	CURR_CV
SCREEN	1.00000 0.0 114	-0.65879 0.0001 114	0.07085 0.4538 114	-0.40304 0.0001 114	0.20211 0.0310 114	0.03652 0.6997 114	0.03652 0.6997 114	0.11967 0.3132 73	-0.31054 0.0075 73
SCRNPORE	-0.65879 0.0001 114	1.00000 0.0 114	-0.01081 0.9092 114	0.44231 0.0001 114	-0.09742 0.3025 114	-0.01737 0.8545 114	-0.01737 0.8545 114	-0.19705 0.0947 73	0.35367 0.0021 73
HOURBEG	0.07085 0.4538 114	-0.01081 0.9092 114	1.00000 0.0 114	-0.05951 0.5294 114	0.20840 0.0261 114	0.03606 0.7032 114	0.03606 0.7032 114	0.08184 0.4912 73	-0.00784 0.9475 73
UNITLOAD	-0.40304 0.0001 114	0.44231 0.0001 114	-0.05951 0.5294 114	1.00000 0.0 114	0.00372 0.9686 114	0.37806 0.0001 114	0.37806 0.0001 114	0.22104 0.0602 73	0.15951 0.1777 73
R_PERMIN	0.20211 0.0310 114	-0.09742 0.3025 114	0.20840 0.0261 114	0.00372 0.9686 114	1.00000 0.0 114	0.09790 0.3001 114	0.09790 0.3001 114	0.08193 0.4907 763	-0.04022 0.7355 73
CURR_ANG	0.03652 0.6997 114	-0.01737 0.8545 114	0.03606 0.7032 114	0.37806 0.0001 114	0.09790 0.3001 114	1.00000 0.0 114	1.00000 0.0 114	0.91863 0.0001 73	-0.08463 0.4766 73
CUR_ANG9	0.03652 0.6997 114	-0.01737 0.8545 114	0.03606 0.7032 114	0.37806 0.0001 114	0.09790 0.3001 114	1.00000 0.0 114	1.00000 0.0 114	0.91863 0.0001 73	-0.08463 0.4766 73
CUR_ANCV	0.11967 0.3132 73	-0.19705 0.0947 73	0.08184 0.4912 73	0.22104 0.0602 73	0.08193 0.4907 73	0.91863 0.0001 73	0.91863 0.0001 73	1.00000 0.0 73	-0.47144 0.0001 73
CURR_CV	-0.31054 0.0075 73	0.35367 0.0021 73	-0.00784 0.9475 73	0.15951 0.1777 73	-0.04022 0.7355 73	-0.08463 0.4766 73	-0.08463 0.4766 73	-0.47144 0.0001 73	1.00000 0.0 73

Effects of ESBS Local Hydrodynamic Conditions

Data tabulation and analysis of variance

Summaries of different impingement/entrainment variables by camera location, current angle, velocity and beginning time are presented in Table 5 with associated statistics in Table 6. This analysis was restricted to the ESBS because too few hydraulic physical modeling observations were available for the ESTS. Also, there were only 18 observations (comprising 59 impingement behavior events) in which we had impingement behavior data collected with the same design and deployment alternatives as were used for the physical modeling. The results are restricted to camera locations 21 through 38, since we had no observations from camera locations 2 and 13. We also had to use replicates that had as few as one smolt to have sufficient data to analyze. Consequently, the results of this section should be viewed as being preliminary; however, they are generally consistent with findings from the McNary Dam analysis (Nestler and Davidson in preparation).

Note the pattern of increases in the R_IMPNGD and R_IMPNGI indices at camera location 21. The highest values of R_IMPNGD (Table 5) are associated with water approach angles nearly perpendicular (10 deg off perpendicular) to the screen surface (the ratio of impinged fishes to the total observed is 0.21 contrasted to about 0.05 for the shallower approach angles (P=0.00001, Table 6). R_IMPNGI shows the same pattern of higher rate with steeper angle as the impingement proportion variable, although the probability is less significant (P=0.0170, Table 6).

The effect of water velocity is less conclusive because of the narrow range of velocities (2.0 and 2.5 fps) that were available for analysis. There was no significant effect of velocity (Table 5) on impingement index (R_IMPNGI, P = 0.2426, Table 6)). However, increased velocity (Table 5) resulted in a significant increase (P = 0.0006, Table 6) in impingement proportion (R_IMPNGD).

R_IMPNGI and R_IMPNGD indices were significantly affected by local hydrodynamic conditions (seven significant entries, Table 6). However, the passage indices were less affected by local hydrodynamic conditions as indicated by the reduced number of significant entries in Table 6 under the passage variables R_IMPNEN and R_IMPNGN (1 significant entry).

Beginning time appears to affect patterns in several of the variables (Table 5). Beginning time has a significant effect on entrainment without screen contact (R_IMPNEN, P = 0.0803, Table 6), imaging rate (R_PERMIN, P = 0.0810, Table 6), and escape after contact (R_IMPNES, P = 0.0176). Its effect on the impingement variables (R_IMPNGD and R_IMPNGI) are much less (P = 0.4044 and 0.1942, respectively) than the effects of the hydrodynamic variables and camera location.

Table 5
Proportions of Smolts on the ESBS Responding only to Different Localized Hydrodynamic Conditions at the Dalles Using Velocities and Angles Extrapolated from Physical Models

SUMMARY PROPORTIONS BY CAMERA LOCATION								
CAMLOC	FREQ	R_IMPNGH	R_IMPNGI	R_IMPNGD	R_IMPNGN	R_IMPNEN	R_IMPNES	R_PERMIN
21	5	0.00000	0.53333	0.28571	0.00000	0.21905	0.36667	0.02475
26	8	0.03125	0.24271	0.05625	0.15000	0.57083	0.28542	0.03060
31	3	0.0000	0.37500	0.04167	0.33333	0.29167	0.58333	0.03093
38	2	0.00000	0.35000	0.00000	0.35000	0.30000	0.70000	0.02952
SUMMARY PROPORTIONS BY ANGLE								
CR_ANGRD	FREQ	R_IMPNGH	R_IMPNGI	R_IMPNGD	R_IMPNGN	R_IMPNEN	R_IMPNES	R_PERMIN
10	7	0.03571	0.46071	0.20714	0.27143	0.28571	0.40714	0.02369
30	11	0.00000	0.29167	0.05032	0.09091	0.46699	0.40152	0.03223
SUMMARY PROPORTIONS BY VELOCITY CATEGORIES								
CR_VELRD	FREQ	R_IMPNGH	R_IMPNGI	R_IMPNGD	R_IMPNGN	R_IMPNEN	R_IMPNES	R_PERMIN
2.0	9	0.02778	0.37222	0.06389	0.32222	0.31944	0.51111	0.02780
2.5	9	0.00000	0.34259	0.15873	0.00000	0.47354	0.29630	0.02003
SUMMARY PROPORTIONS BY HOURBEGIN								
HOURBEG	FREQ	R_IMPNGH	R_IMPNGI	R_IMPNGD	R_IMPNGN	R_IMPNEN	R_IMPNES	R_PERMIN
20	10	0.00000	0.33917	0.17536	0.14000	0.49702	0.21833	0.036328
22	8	0.03125	0.38021	0.03125	0.18750	0.27083	0.63542	0.019643

Note: Hydrodynamic variables had to rounded to the nearest 0.5 fps for velocity and to the nearest 20 deg for the angle of the flow to the screen to minimize the degrees of freedom of the analysis.

Table 6
Summary of Analysis of Variance for ESBS only for Effects of Localized Hydrodynamic Variables on Smolt Entrainment and Impingement Behavior

Combined Analysis							
SOURCE	R_PERMIN	R_IMPNEN	R_IMPNES	R_IMPNGI	R_IMPNGH	R_IMPNGN	R_IMPNGD
COMBINED	0.5344	0.1368	0.1011	0.0270	0.6724	0.6969	0.0012
CR_ANGRD	0.2383	0.2702	0.4911	0.0101	0.8380	0.9500	0.0001
CR_VELRD	0.5354	0.9689	0.3478	0.1604	0.5841	0.5769	0.0013
HOURBEG	0.0810	0.0803	0.0176	0.1942	0.3491	0.7700	0.4044
CAMLOC	0.6437	0.0832	0.4320	0.0114	0.7119	0.9979	0.0022
N	18	18	18	18	18	18	18
ENTRAINMENT SAMPLES - DURATION = 1998 MINUTES : TOT_SEEN = 59 SMOLTS : RATE_SEEN = 0.029530 SMOLTS/MINUTE							

Note: Summaries below table provide sampling information including number of replicates and smolts, duration of sampling, and rate smolts were imaged.

Regression analysis

Multiple regression equations predicting the impingement behavior of smolts are presented in Table 7. Predictive equations having an R^2 of approximately 0.25 were found for impingement proportion (R_IMPNGD, $R^2 = 0.2889$) and headfirst entrainment without screen contact (R_IMPNGN, $R^2 = 0.2508$). While these values are too low for use in design studies, they are high enough to suggest that more refined studies, increased number of observations, and increased compatibility of the physical hydraulic modeling scenarios and videoimaging conditions may allow development of more robust equations having design value. Development of improved methods for describing hydrodynamic variables using video imaging would probably lead to increased R^2 values. For example, meters that measure water velocity and water approach angle at the location of the cameras would probably increase the utility of the impingement data.

Table 7
Summary of Multiple Regression Analysis Using Backward Elimination of Entrainment and Impingement Variables Against Select Hydrodynamic Variables for the ESBS only

Dependent Variables	R-square	DF reg/err/tot	Equation Prob > F	Independent Variables	Parameter Estimates	Individual Probabilities
R_PERMIN		No statistically significant model found				
R_IMPNEN		No statistically significant model found				
R_IMPNES		No statistically significant model found				
R_IMPNGI		No statistically significant model found				
R_IMPNGH		No statistically significant model found				
R_IMPNGN	0.2508	1/16/17	0.0343	INTERCEP CR_VELRD	1.6111111 -0.6444444	0.0212 0.0343
R_IMPNGD	0.2889	3/28/31	0.0556	INTERCEP CR_ANGRD CAMLOC CR_VELRD	0.9975216 -0.0056054 -0.0234984 0.0939270	0.0115 0.0569 0.0428 0.0938

Effects of ESTS Local Hydrodynamic Conditions

Data tabulation and analysis of variance

Summaries of different impingement/entrainment variables by camera location, current angle, velocity, and beginning time are presented in Table 8, with associated statistics in Table 9. This analysis was restricted to the ESTS for data compatibility reasons. Too few hydraulic physical modeling

Table 8
Proportions of Smolts on the ESTS Responding only to Different Localized Hydrodynamic Conditions at The Dalles Dam Using Angles and Standard Deviations of Angles Measured from the Videoimaging

SUMMARY PROPORTIONS BY CAMERA LOCATION

CAMLOC	FREQ	R_IMPNGH	R_IMPNGI	R_IMPNGD	R_IMPNGN	R_IMPNEN	R_IMPNES	FREQ	R_PERMIN
2	1	0.00000	0.12500	0.00000	0.25000	0.75000	0.25000	4	0.01855
13	6	0.00000	0.22738	0.00000	0.04762	0.54524	0.35476	8	0.03125
21	2	0.00000	0.35417	0.00000	0.00000	0.29167	0.45833	12	0.01480
26	6	0.05555	0.33333	0.05556	0.00000	0.38889	0.22222	14	0.01838
31	4	0.00000	0.06250	0.03125	0.00000	0.90625	0.06250	9	0.02508
38	1	0.00000	0.30000	0.00000	0.00000	0.40000	0.40000	8	0.02710

SUMMARY PROPORTIONS BY ANGLE

CR_ANGRD	FREQ	R_IMPNGH	R_IMPNGI	R_IMPNGD	R_IMPNGN	R_IMPNEN	R_IMPNES	FREQ	R_PERMIN
100	0							2	0.00840
110	0							3	0.01121
120	6	0.00000	0.25000	0.00000	0.00000	0.50000	0.16667	19	0.01748
130	12	0.02778	0.25188	0.03819	0.02381	0.53442	0.31905	25	0.02747
140	1	0.00000	0.10000	0.00000	0.00000	0.80000	0.20000	2	0.02917
150	1	0.00000	0.12500	0.00000	0.25000	0.75000	0.25000	2	0.01856

(Continued)

Note: Hydrodynamic variables had to rounded to the nearest 0.5 fps for velocity and to the nearest 20 deg for the angle of the flow to the screen to minimize the degrees of freedom of the analysis, i.e., there were too few observations to further subset either variable without losing the replication necessary to perform ANOVA.

Table 8 (Concluded)

SUMMARY PROPORTIONS BY STANDARD DEVIATION OF WATER APPROACH ANGLE									
CURR_ANG	FREQ	R_IMPNGH	R_IMPNGI	R_IMPNGD	R_IMPNGN	R_IMPNEN	R_IMPNES	FREQ	R_PERMIN
	0							22	0.01249
0	12	0.02778	0.24167	0.02778	0.02083	0.54444	0.25833	20	0.02670
10	8	0.00000	0.23095	0.01563	0.03571	0.55372	0.27232	13	0.03090
SUMMARY PROPORTIONS BY HOURBEGIN									
HOURBEG	FREQ	R_IMPNGH	R_IMPNGI	R_IMPNGD	R_IMPNGN	R_IMPNEN	R_IMPNES	FREQ	R_PERMIN
20	11	0.03030	0.27327	0.03030	0.02597	0.48377	0.31926	30	0.01862
22	9	0.00000	0.19352	0.01389	0.02778	0.62685	0.19630	25	0.02572

Table 9
Summary of Analysis of Variance for ESTS only for Effects of Localized Hydrodynamic Variables on Smolt Entrainment and Impingement Behavior

COMBINED ANALYSIS							
SOURCE	R_PERMIN	R_IMPNEN	R_IMPNES	R_IMPNGI	R_IMPNGH	R_IMPNGN	R_IMPNGD
COMBINED	0.6814	0.8926	0.6871	0.8955	0.8155	0.0543	0.9190
CURR_ANG	0.4070	0.8558	0.4972	0.8028	0.7978	0.0180	0.7720
CURR_CV	0.6506	0.7299	0.8530	0.6463	0.3535	0.3488	0.5832
UNITLOAD	0.8810	0.5595	0.2983	0.6443	0.4391	0.2666	0.7345
N	20	20	20	20	20	20	20
ENTRAINMENT SAMPLES - DURATION = 2380 MINUTES : TOT_SEEN =85 SMOLTS : RATE_SEEN = 0.035714 SMOLTS/MINUTE							

Note: Summaries at bottom provide sampling information including number of replicates and smolts, duration of sampling, and the rate smolts were imaged.

observations were available for the ESTS so that the only data available for the ESTS analysis were data obtained from the videoimaging. The water approach angle (CURR_ANG) and standard deviation of water approach angle (CURR_CV), a surrogate for turbulence, were the two hydrodynamic variables used in the analysis. Unitload is employed as a crude surrogate for water velocity because insufficient physical model data were available. Because of these data limitations, the results of this section should be viewed as being preliminary.

Only one statistically significant relationship was observed at $\alpha=0.20$. The proportion of smolts moving headfirst without screen contact (R_IMPNGN, Table 8) was greatest at a water angle of 150 deg ($P = 0.0180$, Table 9).

Regression analysis

Multiple regression equations predicting the impingement behavior of smolts are presented in Table 7. A statistically significant ($a < 0.05$) predictive equation having an R^2 of approximately 0.25 were found only for the proportion of smolts moving headfirst without screen contact (R_IMPNGN). However, this model is based on one positive result from a single water approach angle (150°, Table 8). No useful regression models were identified because of inadequate data or because the surface of an ESTS supports a much more complex hydrodynamic environment that may require a better hydrodynamic description before the responses of fishes can be understood (Table 10). Development of improved methods for describing and assessing hydrodynamic variables using video imaging would probably lead to increased R^2 values, although traveling screens may inherently provide a more variable hydrodynamic environment than bar screens limiting our ability to develop simple relationships between impingement and localized hydrodynamic conditions.

Screen Porosity

Summaries of the data indicated that there were insufficient observations for analysis of one of the two porosities for each screen design. For the ESBS there were 18 observations for the 50-percent porosity perforation plate, but only 2 observations for the 45-percent screen porosity (Table 11). Similarly, for the ESTS there 17 observations for the 54-percent porosity, but only 2 observations for the 45-percent porosity (Table 12).

Camera Location and Unitload

The effects of camera location and unitload (Table 13), beginning time (Table 14), and screen type (Table 15) were evaluated.

Table 10
Summary of Multiple Regression Analysis Using Backward Elimination of Entrainment and Impingement Variables Against Select Hydrodynamic Variables for the ESTS only

Dependent Variable	R-square	DF reg/err/tot	Equation Prob > F	Independent Variables	Parameter Estimates	Individual Probabilities
R_PERMIN		No statistically significant model found				
R_IMPNEN		No statistically significant model found				
R_IMPNES		No statistically significant model found				
R_IMPNGI		No statistically significant model found				
R_IMPNGH		No statistically significant model found				
R_IMPNGN	0.2460	1/18/19	0.0261	INTERCEP CURR_ANG	-0.6800948 0.0055010	0.0212 0.0261
R_IMPNGD		No statistically significant model found				

Table 11
Summary of Screen Porosity Effects on Select Hydraulic Variables for the ESBS

SCRNPORE	_FREQ_	CURR_ANG	CUR_ANG9	CRAN9_CV	CURR_CV
45	2	115.0	25.0	25.0	0
50	20	127.5	37.5	35.5	2

Note: For the ESBS there were only two replicates for porosity for the 45-percent screen and 20 replicates for 50-percent screen. The number of replicates for the 45-percent screen is too small a sample size for evaluation of the effects of screen porosity on either hydrodynamic variables or impingement behavior variables.

Table 12
Summary of Screen Porosity Effects on Select Hydraulic Variables for the ESTS

SCRNPORE	_FREQ_	CURR_ANG	CUR_ANG9	CRAN9_CV	CURR_CV
45	2	135.000	45.0000	45.0000	0.00000
54	18	127.778	37.7778	33.3333	4.44444

Note: For the ESTS there were only two replicates for porosity for the 45-percent screen and 18 replicates for 54-percent screen. The number of replicates for the 45-percent screen is too small a sample size for evaluation of the effects of screen porosity on either hydrodynamic variables or impingement behavior variables.

Table 13
Proportions of Spring-Time Smolts Exhibiting Different Types of Impingement Behaviors by Camera Location for The Dalles Dam for Screen Types, Unitload, Screen Porosity, and Beginning Times Combined

SUMMARY PROPORTIONS BY CAMERA LOCATION

CAMLOC	FREQ	R_IMPNGH	R_IMPNGI	R_IMPNGD	R_IMPNGN	R_IMPNEN	R_IMPNES	FREQ	R_PERMIN	CURR_ANG	CUR_ANG9	CRAN9_CV	CURR_CV
2	3	0.000000	0.23611	0.000000	0.083333	0.52778	0.36111	14	0.027211	142.857	52.8571	50.0000	2.50000
13	9	0.000000	0.21640	0.000000	0.031746	0.56720	0.27354	18	0.033495	133.333	43.3333	40.6667	3.33333
21	8	0.000000	0.40104	0.095238	0.000000	0.29315	0.44792	29	0.026171	125.862	35.8621	35.3333	1.33333
26	10	0.058333	0.31917	0.078333	0.020000	0.44000	0.21167	25	0.022686	118.000	28.0000	27.5000	1.87500
31	10	0.010000	0.16224	0.038846	0.015385	0.70051	0.16538	18	0.063335	124.444	34.4444	32.0000	3.33333
38	2	0.000000	0.25000	0.000000	0.10000	0.50000	0.40000	10	0.027585	119.000	29.0000	25.0000	2.50000

SUMMARY PROPORTIONS BY UNITLOAD - ALL CAMERAS COMBINED

UNITLOAD	FREQ	R_IMPNGH	R_IMPNGI	R_IMPNGD	R_IMPNGN	R_IMPNEN	R_IMPNES	FREQ	R_PERMIN	CURR_ANG	CUR_ANG9	CRAN9_CV	CURR_CV
11	0							1	0.008333	130.000	40.0000		
12	8	0.031250	0.30417	0.12545	0.050000	0.51711	0.22083	24	0.024491	113.750	23.7500	24.2857	1.42857
13	17	0.019608	0.26308	0.04148	0.023756	0.51305	0.32376	49	0.036586	129.592	39.5918	37.8125	2.50000
14	8	0.012500	0.23125	0.01250	0.000000	0.53750	0.20833	14	0.052757	135.714	45.7143	43.3333	1.66667
15	9	0.000000	0.26918	0.01389	0.031746	0.47553	0.30688	26	0.023016	127.692	37.6923	32.6667	4.00000

SUMMARY PROPORTIONS BY UNITLOAD - CAMERA LOCATION 2 ONLY

13	2	0	0.22917	0	0.125	0.54167	0.29167	6	0.034166	141.667	51.6667	50.0000	2.50000
14	1	0	0.25000	0	0.000	0.50000	0.50000	5	0.027018	140.000	50.0000	46.6667	3.33333
15	0							3	0.013624	150.000	60.0000	60.0000	0.00000

(Continued)

Note: For both screen types, fyke nets were not deployed, no closure gate was present, and the screens were at the standard elevation. Beginning time is rounded to the nearest 2 hours and unitload is rounded to the nearest 1 kcfs. A total of 114 replicates were made of the hydrodynamic variables and 42 replicates were evaluated for the impingement behavior variables.

Table 13 (Concluded)

SUMMARY PROPORTIONS BY UNITLOAD - CAMERA LOCATION 13 ONLY												
13	3	0	0.24444	0	0.000000	0.51111	0.28889	11	0.024188	132.727	42.7273	41.2500	2.50000
14	3	0	0.19444	0	0.000000	0.61111	0.11111	4	0.055044	137.500	47.5000	45.0000	2.50000
15	3	0	0.21032	0	0.095238	0.57937	0.42063	3	0.038889	130.000	40.0000	33.3333	6.66667
SUMMARY PROPORTIONS BY UNITLOAD - CAMERA LOCATION 21 ONLY												
11	0	-	-	-	-	-	-	1	0.008333	130.000	40.0000		
12	2	0	0.33333	0.21429	0	0.54762	0.16667	6	0.023450	118.333	28.3333	26.6667	0.00000
13	4	0	0.41667	0.08333	0	0.25000	0.66667	15	0.025715	127.333	37.3333	37.1429	1.42857
14	1	0	0.50000	0.00000	0	0.00000	0.33333	2	0.066667	130.000	40.0000	40.0000	0.00000
15	1	0	0.37500	0.00000	0	0.25000	0.25000	5	0.018175	128.000	38.0000	36.6667	3.33333
SUMMARY PROPORTIONS BY UNITLOAD - CAMERA LOCATION 26 ONLY												
12	4	0.06250	0.29792	0.11250	0.05	0.51667	0.19583	11	0.025314	113.636	23.6364	27.1429	0.00000
13	3	0.11111	0.27778	0.11111	0.00	0.55556	0.11111	9	0.021892	122.222	32.2222	28.3333	3.33333
15	3	0.00000	0.38889	0.00000	0.00	0.22222	0.33333	5	0.018333	120.000	30.0000	26.6667	3.33333
SUMMARY PROPORTIONS BY UNITLOAD - CAMERA LOCATION 31 ONLY												
12	1	0.000000	0.37500	0.12500	0.000000	0.37500	0.25000	3	0.030932	113.333	23.3333	20.0	5.00000
13	4	0.000000	0.12019	0.00962	0.038462	0.75962	0.16346	7	0.093653	128.571	38.5714	35.0	3.33333
14	3	0.033333	0.17222	0.03333	0.000000	0.65556	0.16667	3	0.083333	130.000	40.0000	40.0	0.00000
15	2	0.000000	0.12500	0.06250	0.000000	0.81250	0.12500	5	0.028333	122.000	32.0000	27.5	5.00000
SUMMARY PROPORTIONS BY UNITLOAD - CAMERA LOCATION 38 ONLY												
12	1	0.0	0.2	0.0	0.2	0.6	0.4	4	0.018962	107.5	17.5	15	5
13	1	0.0	0.3	0.0	0.0	0.4	0.4	1	0.083333	130.0	40.0	40	0
15	0	-						5	0.023333	126.0	36.0	30	0

Table 14
Proportions of Spring-Time Smolts Exhibiting Different Types of Impingement Behaviors by Beginning Time for The Dalles Dam for Screen Types, Unitloads, Screen Porosities, and Screen Types Combined

SUMMARY PROPORTIONS BY BEGINNING TIME - ALL CAMERAS COMBINED												
HOURBEG	FREQ	R_IMPNGH	R_IMPNGI	R_IMPNGD	R_IMPNGN	R_IMPNEN	R_IMPNES	FREQ	R_PERMIN	CURR_ANG	CUR_ANG9	CRAN9_CV	CURR_CV
20	22	0.019697	0.26883	0.053950	0.031169	0.51174	0.29675	58	0.022086	126.207	36.2069	34.1667	2.50000
22	20	0.012500	0.26321	0.037340	0.020192	0.50901	0.25853	56	0.043659	126.964	36.9643	35.9459	2.43243
SUMMARY PROPORTIONS BY BEGINNING TIME - CAMERA LOCATION 2 ONLY													
HOURBEG	FREQ	R_IMPNGH	R_IMPNGI	R_IMPNGD	R_IMPNGN	R_IMPNEN	R_IMPNES	FREQ	R_PERMIN	CURR_ANG	CUR_ANG9	CRAN9_CV	CURR_CV
20	0	-	-	-	-	-	-	8	0.011533	142.500	52.5000	53.3333	0
22	3	0	0.23611	0	0.083333	0.52778	0.36111	6	0.048116	143.333	53.3333	48.0000	4
SUMMARY PROPORTIONS BY BEGINNING TIME - CAMERA LOCATION 13 ONLY													
20	4	0	0.26190	0	0.071429	0.47619	0.39881	10	0.023333	133.00	43.0000	40.0000	3.75000
22	5	0	0.18000	0	0.000000	0.64000	0.17333	8	0.046197	133.75	43.7500	41.4286	2.85714
SUMMARY PROPORTIONS BY BEGINNING TIME - CAMERA LOCATION 21 ONLY													
20	5	0	0.37500	0.08571	0	0.33571	0.45000	13	0.019980	123.846	33.8462	35.7143	0.0
22	3	0	0.44444	0.11111	0	0.22222	0.44444	16	0.031201	127.500	37.5000	35.0000	2.5
SUMMARY PROPORTIONS BY BEGINNING TIME - CAMERA LOCATION 26 ONLY													
20	7	0.047619	0.29524	0.076190	0.028571	0.48571	0.21905	13	0.023881	119.231	29.2308	30.0000	1.11111
22	3	0.083333	0.37500	0.083333	0.000000	0.33333	0.19444	12	0.021391	116.667	26.6667	24.2857	2.85714
SUMMARY PROPORTIONS BY BEGINNING TIME - CAMERA LOCATION 31 ONLY													
20	5	0.02	0.14500	0.045000	0.000000	0.73500	0.15000	9	0.033459	122.222	32.2222	27.5000	5.00000
22	5	0.00	0.17949	0.032692	0.030769	0.66603	0.18077	9	0.093212	126.667	36.6667	37.1429	1.42857
SUMMARY PROPORTIONS BY BEGINNING TIME - CAMERA LOCATION 38 ONLY													
20	1	0	0.2	0	0.2	0.6	0.4	5	0.016808	118	28	10	10
22	1	0	0.3	0	0.0	0.4	0.4	5	0.038362	120	30	30	0

Note: For both screen types, a fyke net was deployed, no gate was present, and the screens were at the standard elevation and the standard angle. Unitload is rounded to the nearest 2 hr and unitload is rounded to the nearest 1 kcfs. A total of 104 replicates were made of the hydrodynamic variables and 40 replicates were evaluated for the impingement behavior variables.

Table 15

Proportions of Spring-Time Smolts Exhibiting Different Types of Impingement Behaviors by Screen Type for The Dalles Dam for Screen Types, Unitloads, Screen Porosities, and Beginning Times Combined

SUMMARY PROPORTIONS BY SCREEN TYPE - ALL CAMERAS COMBINED												
SCRNTYPE	FREQ	R_IMPNGH	R_IMPNGI	R_IMPNGD	R_IMPNGN	R_IMPNEN	R_IMPNES	FREQ	R_PERMIN	CURR_ANG	CUR_ANG9	CRAN9_CV	CURR_CV
E	20	0.016667	0.23738	0.022917	0.026786	0.54815	0.26393	55	0.021850	126.182	36.1818	33.6364	3.93939
X	22	0.015909	0.29231	0.067062	0.025175	0.47615	0.29184	59	0.042782	126.949	36.9492	36.2500	1.25000
SUMMARY PROPORTIONS BY SCREEN TYPE - CAMERA LOCATION 2 ONLY												
SCRNTYPE	FREQ	R_IMPNGH	R_IMPNGI	R_IMPNGD	R_IMPNGN	R_IMPNEN	R_IMPNES	FREQ	R_PERMIN	CURR_ANG	CUR_ANG9	CRAN9_CV	CURR_CV
E	1	0	0.12500	0	0.25	0.75000	0.25000	4	0.018552	150	60	60.0000	0.00000
X	2	0	0.29167	0	0.00	0.41667	0.41667	10	0.030675	140	50	46.6667	3.33333
SUMMARY PROPORTIONS BY SCREEN TYPE - CAMERA LOCATION 13 ONLY												
E	6	0	0.22738	0	0.047619	0.54524	0.35476	8	0.031250	132.500	42.5000	37.1429	5.71429
X	3	0	0.19444	0	0.000000	0.61111	0.11111	10	0.035291	134.000	44.0000	43.7500	1.25000
SUMMARY PROPORTIONS BY SCREEN TYPE - CAMERA LOCATION 21 ONLY												
E	2	0	0.35417	0.00000	0	0.29167	0.45833	12	0.014807	128.333	38.3333	36	4
X	6	0	0.41667	0.12698	0	0.29365	0.44444	17	0.034193	124.118	34.1176	35	0
SUMMARY PROPORTIONS BY SCREEN TYPE - CAMERA LOCATION 26 ONLY												
E	6	0.055556	0.33333	0.05556	0.00	0.38889	0.22222	14	0.018379	117.857	27.8571	26.6667	3.33333
X	4	0.062500	0.29792	0.11250	0.05	0.51667	0.19583	11	0.028167	118.182	28.1818	28.5714	0.00000
SUMMARY PROPORTIONS BY SCREEN TYPE - CAMERA LOCATION 31 ONLY												
E	4	0.000000	0.06250	0.031250	0.000000	0.90625	0.06250	9	0.025080	124.444	34.4444	30.0000	5.00000
X	6	0.016667	0.22874	0.043910	0.025641	0.56335	0.23397	9	0.101590	124.444	34.4444	34.2857	1.42857
SUMMARY PROPORTIONS BY SCREEN TYPE - CAMERA LOCATION 38 ONLY												
E	1	0	0.3	0	0.0	0.4	0.4	8	0.027101	121.250	31.2500	35	0
X	1	0	0.2	0	0.2	0.6	0.4	2	0.029520	110.000	20.0000	15	5

Note: For both screen types, a fyke net was deployed, no gate was present, and the screens were at the standard elevation and the standard angle. Unitload is rounded to the nearest 2 hr and unitload is rounded to the nearest 1 kcfs. A total of 104 replicates were made of the hydrodynamic variables and 40 replicates were evaluated for the impingement behavior variables. E=EXTENDED TRAVELING SCREEN X=EXTENDED BAR SCREEN

Table 13 presents tabular summaries for the effects of camera location and unitload on impingement/passage characteristics and hydrodynamic variables. This analysis was also affected by relatively low numbers of observations, particularly for camera locations 2 and 38. The paucity of data will influence those variables that are most data intensive (e.g., impingement index, R_IMPNGD).

Camera location

Table 13 (top block) provides summaries by camera location for screen design, screen porosity, unitload, and beginning times combined. Several statistically significant (at $\alpha = 0.05$ and $\alpha = 0.20$) relationships were observed between camera location and the impingement/passage variables. Imaging rate was about twice as high at camera location 31 (0.06 smolts per minute) as at the other camera locations (P = 0.1392, Table 16). Impingement index (R_IMPNGI, Table 13) was highest at cameras 21 and 26 (P = 0.0849, Table 16) and the passage without screen contact (R_IMPNEN, Table 13) was lowest at the middle cameras by about a factor of 2 (0.0527). Water approach angle (CURR_ANG, Table 13) was heavily influenced by camera location (P = 0.0001, Table 16). However, the standard deviation of water angle (CURR_CV, Table 13) was not affected by camera location (P = 0.7673, Table 16).

Unitload

The second block of Table 13 presents summaries by unitload for all camera locations combined. The remainder of Table 13 presents summaries by unitload for the different camera locations. Unitload does not have a statistically significant effect (at $\alpha = 0.05$) or consistent effect on any of the impingement behavior variables - possibly because the different screen designs were tested under different unitloads. One impingement behavior variable, escape after screen contact (R_IMPNES) has a statistically significant effect at P = 0.0815 (Table 16), but the pattern is not consistent across the range of unitloads tested. Unitload affected average water approach angle (CURR_ANG, Table 13) but did not affect the standard deviation of water approach angle (CURR_CV, Table 13).

Relatively few significant relationships (4 out of 42 possible) were observed for the impingement behavior variables at each specific camera location. No consistent patterns could be discerned. There appeared to be several significant relationships between unitload and hydrodynamic variables at most of the camera locations. However, unitloads tended to be specific to each screen design tested so that unitload and screen design were probably confounded.

Table 16
Summary of Analysis of Variance for Effects of Screen Type, Unitload, and Camera Location on Entrainment and Hydrodynamic Variables

COMBINED ANALYSIS

SOURCE	R_PERMIN	R_IMPNGH	R_IMPNGI	R_IMPNGD	R_IMPNGN	R_IMPNEN	R_IMPNES	CURR_ANG	CUR_ANG9	CRAN9_CV	CURR_CV
COMBINED	0.0566	0.7377	0.1838	0.5144	0.5702	0.1306	0.0760	0.0001	0.0001	0.0001	0.4789
SCRNTYPE	0.0651	0.6832	0.1409	0.8718	0.7126	0.0831	0.0377	0.9835	0.9835	0.4828	0.0417
UNITLOAD	0.7824	0.6986	0.6314	0.4141	0.4923	0.2650	0.0815	0.0001	0.0001	0.0071	0.9105
CAMLOC	0.1392	0.4472	0.0849	0.7017	0.2657	0.0527	0.1278	0.0001	0.0001	0.0009	0.7673
HOURBEG	0.0555	0.9285	0.5752	0.7313	0.5274	0.6364	0.5093	0.6422	0.6422	0.7581	0.7436
N	114	42	42	42	42	42	42	114	114	114	114

ENTRAINMENT SAMPLES - DURATION = 4,447 MINUTES : TOT_SEEN=221 SMOLTS : RATE_SEEN=0.02777 SMOLTS/MINUTE
Hydrodynamic SAMPLES - DURATION = 11,768 MINUTES : MEASUREMENTS=326

CAMERA LOCATION 2 ONLY

SOURCE	R_PERMIN	R_IMPNGH	R_IMPNGI	R_IMPNGD	R_IMPNGN	R_IMPNEN	R_IMPNES	CURR_ANG	CUR_ANG9	CRAN9_CV	CURR_CV
UNITLOAD	0.5920	0	0.9268	0	0	0.9268	0.2123	0.0011	0.0011	0.3629	0.8668
SCRNTYPE	0.4655	0	0.2601	0	0	0.2601	0.4544	0	0	0.0134	0.4198
N	14	3	3	3	3	3	3	14	14	8	8

ENTRAINMENT SAMPLES - DURATION = 240 MINUTES : TOT_SEEN=14 SMOLTS : RATE_SEEN=0.0220 SMOLTS/MINUTE
Hydrodynamic SAMPLES - DURATION = 1,365 MINUTES : MEASUREMENTS=30

CAMERA LOCATION 13 ONLY

SOURCE	R_PERMIN	R_IMPNGH	R_IMPNGI	R_IMPNGD	R_IMPNGN	R_IMPNEN	R_IMPNES	CURR_ANG	CUR_ANG9	CRAN9_CV	CURR_CV
UNITLOAD	0.0600	0	0.8864	0	0.4219	0.8864	0.3284	0.2298	0.2298	0.2932	0.4488
SCRNTYPE	0.7269	0	0.7045	0	0.5165	0.7045	0.1663	0.6097	0.6097	0.1942	0.0753
N	18	9	9	9	9	9	9	18	18	15	15

ENTRAINMENT SAMPLES - DURATION = 957 MINUTES : TOT_SEEN=41 SMOLTS : RATE_SEEN=0.0304 SMOLTS/MINUTE
Hydrodynamic SAMPLES - DURATION = 1,840 MINUTES : MEASUREMENTS=56

(Continued)

Note: For each variable there were three classes of unitload (12, 14, and 16 kcfs), two screen types (E and X), two beginning times (2000 and 2200 Hours) and six camera locations. Probabilities are based on Type III sum of squares to reduce confounding effects of other variables. The analysis tests the hypothesis that the means of the different entrainment/impingement variables and hydrodynamic variables are not different by the treatment variables. Probabilities less than 0.20 are highlighted to enhance comparability to other tables and to aid in identifying trends. The "COMBINED ANALYSIS" combines variables. However, the analyses by camera location are done individually by variable, because too few observations were available to combine the analysis. Results are presented in combined form for brevity of presentation.

Table 16 (Concluded)

CAMERA LOCATION 21 ONLY

SOURCE	R_PERMIN	R_IMPNGH	R_IMPNGI	R_IMPNGD	R_IMPNGN	R_IMPNEN	R_IMPNES	CURR_ANG	CUR_ANG9	CRAN9_CV	CURR_CV
UNITLOAD	0.2129	0	0.8928	0.7874	0	0.1821	0.0265	0.0332	0.0332	0.0391	0.6872
SCRNTYPE	0.0466	0	0.6493	0.4248	0	0.9921	0.9529	0.1021	0.1021	0.7871	0.0319
N	29	8	8	8	8	8	8	29	29	15	15

ENTRAINMENT SAMPLES - DURATION = 828 MINUTES : TOT_SEEN=35 SMOLTS : RATE_SEEN=0.0223 SMOLTS/MINUTE
Hydrodynamic SAMPLES - DURATION = 2,829 MINUTES : MEASUREMENTS=64

CAMERA LOCATION 26 ONLY

SOURCE	R_PERMIN	R_IMPNGH	R_IMPNGI	R_IMPNGD	R_IMPNGN	R_IMPNEN	R_IMPNES	CURR_ANG	CUR_ANG9	CRAN9_CV	CURR_CV
UNITLOAD	0.7083	0.6056	0.8211	0.5149	0.5283	0.4888	0.2090	0.0276	0.0276	0.9495	0.2764
SCRNTYPE	0.1173	0.9371	0.8100	0.5299	0.2415	0.6037	0.8064	0.9186	0.9186	0.6420	0.1020
N	25	10	10	10	10	10	10	25	25	16	16

ENTRAINMENT SAMPLES - DURATION = 1,176 MINUTES : TOT_SEEN=40 SMOLTS : RATE_SEEN=0.0223 SMOLTS/MINUTE
Hydrodynamic SAMPLES - DURATION = 2,737 MINUTES : MEASUREMENTS=61

CAMERA LOCATION 31 ONLY

SOURCE	R_PERMIN	R_IMPNGH	R_IMPNGI	R_IMPNGD	R_IMPNGN	R_IMPNEN	R_IMPNES	CURR_ANG	CUR_ANG9	CRAN9_CV	CURR_CV
UNITLOAD	0.7804	0.5855	0.4183	0.2969	0.7583	0.5068	0.9804	0.0003	0.0003	0.0493	0.6009
SCRNTYPE	0.1735	0.4468	0.0410	0.7455	0.4468	0.0120	0.2105			0.3988	0.1648
N	18	10	10	10	10	10	10	18	18	15	15

ENTRAINMENT SAMPLES - DURATION = 1,008 MINUTES : TOT_SEEN=76 SMOLTS : RATE_SEEN=0.04689 SMOLTS/MINUTE
Hydrodynamic SAMPLES - DURATION = 1,898 MINUTES : MEASUREMENTS=89

CAMERA LOCATION 38 ONLY

SOURCE	R_PERMIN	R_IMPNGH	R_IMPNGI	R_IMPNGD	R_IMPNGN	R_IMPNEN	R_IMPNES	CURR_ANG	CUR_ANG9	CRAN9_CV	CURR_CV
UNITLOAD	0.0752	0	0	0	0	0	0	0.0024	0.0024	0.3162	0.8165
SCRNTYPE	0.9183							0.2136	0.2136	0.1056	0.4226
N	10	2	2	2	2	2	2	10	10	4	4

ENTRAINMENT SAMPLES - DURATION = 238 MINUTES : TOT_SEEN=15 SMOLTS : RATE_SEEN=0.0238 SMOLTS/MINUTE
Hydrodynamic SAMPLES - DURATION = 1,091 MINUTES : MEASUREMENTS=26

Beginning Time

Summaries of impingement and hydrodynamic variables are presented in Table 14. Imaging rate was highest at 2200 hr (P = 0.0555, Table 16). No other consistent pattern between beginning time and any of the passage/ impingement variables were observed.

Screen Type

Tables 15 and 16 summarize the effects of screen type on impingement/ passage characteristics and hydrodynamic variables. Table 15 presents summaries of data by screen type for all camera locations combined and for each camera location separately. For the combined analysis, screen type had a significant effect at $a < 0.05$ for four of the seven impingement behavior variables. Imaging rate was about double (top block Table 15) on the bar screen than it was on the traveling screen (P = 0.0651, Table 16). Both impingement index (R_IMPNGI) and impingement proportion (R_IMPNGD) were higher on the bar screen than on the traveling screen, although only impingement index was statistically significant (P = 0.1409). Impingement proportion was three times higher on the bar screen than on the traveling screen but highly variable in both cases. Consistent with the impingement variables, passage without screen contact (R_IMPNEN) was highest on the traveling screen (P = 0.0831), and screen contact with subsequent escape (R_IMPNES) was highest on the bar screen. Screen design did not affect water approach angle (CURR_ANG); however, it did affect the standard deviation of the water approach angle (CURR_CV, Table 15). Water approach angles had about three times higher standard deviation on the traveling screen than on the bar screen (P = 0.0417, Table 16). Water flow appears to be more turbulent on the traveling screen than on the bar screen. In contrast, water approach angle (CURR_ANG) was determined primarily by unitload.

Differences between screen design at specific locations are presented in Tables 15 and 16. The effect of screen design on imaging rate is concentrated at the middle cameras (camera locations 21, 26, and 31) with probabilities ranging from P = 0.0466 at camera location 21 to P = 0.1735 at camera location 31. The effect of screen design on the standard deviation of water approach angle also appears to be concentrated in the middle cameras (camera locations 13, 21, 26, and 21) with probabilities ranging from 0.0319 to 0.1648. In all cases the ESTS has a greater standard deviation of water approach angle. No other consistent patterns of impingement behavior or hydrodynamic variables were observed.

5 Discussion

Summary

No conclusions could be reached on the effect of screen porosity. Analysis of screen porosity was limited by inadequate numbers of replicates for the lower perforation plate porosities for each screen design. No consistent, statistically significant effects of unitload were observed.

Attempts to determine the effects of local hydrodynamic conditions on smolt impingement behavior were unsuccessful. Only a few significant relationships were observed and the relationships lacked sufficient R^2 to be of design value.

Analysis of location effects on smolt behavior and hydrodynamic variables was successful. Impingement behavior variables differed by location on the screen. Screen impingement index and screen impingement tended to be highest and passage without screen contact was lowest at the middle camera locations. Hydrodynamic conditions also varied by camera location. Flows were more nearly perpendicular to the screen at its toe (nearest the trashrack) and more parallel to the screen at the top (nearest the draft tube deck).

The screen design analysis provided the most concrete and consistent results from the videoimaging studies. The results from The Dalles when considered with results from the previous year from McNary Dam provided considerable insight into how smolt behavior and hydrodynamic patterns varied between traveling and bar screens.

The screen design analysis provided interesting results that appear to be consistent with the results of the videoimaging results obtained from McNary Dam. The bar rack has higher impingement, higher impingement index, lower entrainment without screen contact, higher escape after contact, higher imaging rate, and lower standard deviation of current angle (a measure of turbulence) than the traveling screen. These results all suggest that smolts are better able to detect and avoid the traveling screen than the bar screen. Increased imaging rate of the bar screens suggests that more of the smolts are in the immediate vicinity of the screen, where they are most likely to be imaged. Concomitantly, if more of the smolts are closer to the screen, then

there should also be an increase in those variables that describe screen contact and impingement and a reduction in those variables that describe passage without screen contact.

Based on the results of the screen design analysis and considering results of the McNary Dam analysis, we offer the Relative Pressure Signature Theory (RPST) as a comprehensive concept of how different screen designs and deployment alternatives can affect smolt impingement behavior. The following explanation of the RPST is composed of two parts. The first part explains how different screen designs or elements that result in major alterations in the turbulent characteristics of water flow through a screen affect fish behavior, e.g., how the impingement behavior elicited by traveling screens compares to that of bar screens. The second part describes how deployment alternatives that do not result in major alterations of the turbulence characteristics of water flow in the intake affect fish behavior, e.g., increases in unitload of a magnitude that produce increases in velocity or a redistribution of the velocity field.

Relative Pressure Signature Theory

Comparing screen designs

Fish live in a fluid environment in which movements of the fluid over rough substrates or movements of biota through the medium generate complex hydrodynamic and acoustic fields. Fishes have evolved an elegant and sophisticated (but incompletely understood) data acquisition system - the octavo-lateralis system - that is able to transduce these pressure patterns into information suitable for neuroprocessing. Much of the behavior patterns of fishes is influenced by information obtained from the octavo-lateralis system. For recent reviews of mechanosensory biology of fishes, see chapters in Atema et al. (1988) and Coombs, Gorner, and Muns (1989). Kalmijn's (1989) chapter in the latter volume is especially concise.

Results from videoimaging suggest that bar screens and mesh screens generate substantially different pressure signatures. Pressure is used in the context of acoustical pressure as is generated by a compressional (propagated) wave, in the context of water particle motion as is generated by any kind of oscillator other than a monopole and in the context of fluid pressure resulting from complex velocity patterns associated with turbulent water flow. As Hawkins (1993) states,

> "Close to a sound source, however, it is not easy to draw a distinction between sound and bulk movements of the medium itself. Local turbulent and hydrodynamic effects occur which involve net motion of the medium, and neither depend upon the elasticity of the medium nor propagate at the velocity of sound...To a particular sense organ, these hydrodynamic effects may be indistinguishable from sounds."

Water approach angles are more variable on traveling screens than they are on bar screens. Qualitative comparison of flow characteristics within about 30 cm of each screen design indicates that the traveling screen is characterized by variable, turbulent flows (even rollers spontaneously appear and disappear on the surface of the mesh screen), whereas the bar screen is characterized by more laminar flow conditions associated with its increased hydrodynamic efficiency. The tiedown bars, woven mesh, and structural members supporting the screen all probably function to create complex and dynamic flow conditions near the screen surface which are of sufficient energy level to be detected by the sound sensory system of fish.

The structural simplicity and increased flow efficiency of the bar screens may produce less extensive and more laminar pressure and velocity fields than do the less hydrodynamically efficient mesh screens. The turbulence generated by the mesh screens may provide the smolts' mechanosensory systems (ears and lateral lines) with necessary information to perceive and localize the obstacle and thereby avoid impingement.

Conversely, smolts are more likely to be struck and injured on the rather unyielding surface of the bar rack. This premise is supported by the increased imaging rate and increased strike frequency of smolts on the bar rack. More fishes seem to be closer to the screen (and hence more likely to imaged or strike) on the bar rack than on the traveling screen. The paucity of statistically significant relationships for the ESTS (1) compared for the ESBS (15) under the local hydrodynamic environment analysis may also be related to the same phenomenon. While part of the reason is because of the data inadequacies within the ESTS, it may be that the ESTS's generate complex pressure and hydrodynamic stimuli that function as extra sets of variables to confound the ESTS analysis.

The small-scale, but intense hydraulic features on the mesh screen surface are probably generated by large-scale flow instabilities within the intake. Videoimaging indicates that the bar screen provides relatively little alteration of the flow lines as they are intercepted by the screen. We conclude that the complex flow behavior observed on the surface of the bar screen is not caused by the screen itself but results from large-scale flow instabilities (waves or large-scale turbulence) associated with the detailed geometry of the intake, alignment of the trashrack vanes, and powerhouse and unit effects. The large-scale flow variations produce the intense, smaller-scale flow features observed on the mesh screens as the angle of attack and velocity of the large-scale features changes. The large-scale flow variations efficiently pass through the bar screen relatively unaltered and generate relatively minor pressure signatures as they interact with the bar screen.

The observations made on the relative differences between flow fields of ESBS's and ESTS's can be expanded to include the rest of the hydropower intake environment by using signal-to-noise concepts. The ability of a fish to detect a particular arbitrary signal is partially determined by the strength of the signal relative to the background noise, i.e., the signal-to-noise ratio. A

fish is unable to detect a signal if the strength of the signal is small relative to the level of background noise. This explanation is a major simplification of a complex sensory process.

The idea of the signal-to-noise ratio as one aspect of sensory reception also has application to the behavior of smolts to screens. If, as the evidence suggests, smolts are able to detect the presence of a screen in an intake by its pressure or hydrodynamic signature, then it is also reasonable that the pressure and hydrodyanamic environment within the intake (and perhaps the immediate approach to the trashracks) affects the ability of a smolt to detect the presence of a screen. It seems reasonable, therefore, that the acoustic and hydrodynamic environment in intakes will also partially determine the success of particular screen design or deployment alternatives to guide smolts. Low background noise levels in a laminar flow environment will increase the ability of the smolt to detect and respond to (perhaps even totally avoid) the bypass screen. Although there have been no thorough studies of the acoustic environment within intakes, it seems reasonable that differences in trash rack design or orientation, baynumber, powerhouse configuration, and turbine characteristics could all influence the acoustic and hydrodynamic environment (in a background noise context) and thus have a direct influence on the FGE of a screen. Restated, exactly the same bypass screen design may have substantially different guidance characteristics depending upon the precise blend of factors that together determine the background noise and turbulence characteristics of the intake.

Comparing deployment alternatives

The contrasting near-surface flow characteristics observed qualitatively by videoimaging between traveling and bar screens is more than the differences in flow fields between similar screen designs but operated under different deployment or operational alternatives. For example, increases in unitload or changes in screen porosity on a bar screen do not appear to alter the near field flow characteristics as much as changing screen design. The effects of different deployment or operational alternatives on one screen design can probably be explored and predicted based on mean water velocity and water approach angle because the responses of smolts appears to be simple linear or curvolinear to these conditions. As described for McNary Dam (Nestler and Davidson in preparation), increases in water velocity at the screen surface result in increased impingement and screen contact. Water approach angles that are more perpendicular to the screen surface result in increased impingement and screen contact. However, deployment or operational alternatives that produce major fluctuations in the flow field near the screen surface and produce pressure anomalies that propagate from the screen surface may result in a nonlinear, threshold response by smolts similar to that observed when screen designs were compared.

6 Recommendations

The ability of fishes to detect and respond to pressure and acceleration information is well-documented. This ability is probably employed in a wide variety of normal behaviors that include near-field navigation, predator avoidance, and feeding. Qualitative observations made during videoimaging for both The Dalles and McNary Dams suggest that fish are detecting and responding to the signals being generated by the bypass system. The efficacy of the bypass system is probably at least partially determined by the strength of the signals generated by the bypass system relative to the background noise and turbulence within the intake.

The hydrodynamic environment within the intake appears to generate acoustic/hydrodynamic signals that lie within the sensory ability of smolts, and smolts, in turn, appear to exhibit significant responses to screen design or deployment alternatives. Selection of design alternatives and operational alternatives require a better understanding of the sensory capabilities of smolts relative to the signals available within the intake. We recommend that studies be initiated to characterize the responses of smolts to complex hydrodynamic environments in a natural channel (preferred) or flume of the same approximate scale as an intake. The hydrodynamic environment must be characterized in a manner consistent with the spatio-temporal scale and sensitivity of the smolts sensory system. The characterization must include both detailed descriptions of both the velocity field and the pressure field. The pressure field description must include time varying behavior of both acoustic pressures and velocity pressures associated with turbulent water flow.

We also recommend that the velocity and pressure fields within the intake, including the effects generated by trashracks, splitter walls, and pier noses, be described at the same spatio-temporal scales and precision as are the measurements made in natural or flume channels. Bay, unit location, and siting effects must also be described. The necessary monitoring equipment does not presently exist (research and development of such systems is ongoing at WES) and must be developed as part of these studies.

Integrating the sensory capabilities of smolts and their responses to velocity and acoustic fields, with mappings of the mean and time-varying velocity and pressure fields within and near intakes, will facilitate the design and operation of fish bypass systems.

References

Atema, J. R. R., Fay, R. R., Popper, A. N., and Tavolga, W. N., ed. (1988). *Sensory biology of aquatic animals*. Springer-Verlag, New York, 934.

Coombs, S., Gorner, P., and Muns, H., ed. (1989). *The mechanosensory lateral line*. Springer-Verlag, New York, 936.

Fletcher, Ian. (1985). "Risk analysis for fish diversion experiments: Pumped intake systems." *Transactions of the American Fisheries Society*. 114:652-694.

Hawkins, A. D. (1993). "Underwater sound and fish behaviour." *Behavior of teleost fishes*. T. J. Pitcher, ed., 2nd ed., Chapman & Hall, New York.

Kalmijn, A. J. (1989). "Functional evolution of lateral line and inner ear sensory systems." *The mechanosensory lateral line*. S. Coombs, P. Gorner, and H. Muns, ed., Springer-Verlag, New York, 187-215.

Nestler, J. M., and Davidson, R. (1993). "Imaging smolt behavior on extended-length traveling screens, McNary Dam: 1991 pilot study," Technical Report EL-93-24, U.S. Army Engineer Waterways Experiment Station, Vicksburg, MS.

_____. "Imaging smolt behavior on bypass screens and a vertical barrier screen at McNary Dam in 1992" (technical report in preparation), U.S. Army Engineer Waterways Experiment Station, Vicksburg, MS.

Peterman, R. M. (1990). "Statistical power analysis can improve fisheries research and management," *Can. J. Fish. Aquat. Sci.* 47, 2-14.

SAS Institute, Inc. (1988). "SAS/STAT user's guide," Release 6.03 ed., Cary, NC, 1028.

REPORT DOCUMENTATION PAGE

Form Approved
OMB No. 0704-0188

1. AGENCY USE ONLY (Leave blank)	2. REPORT DATE	3. REPORT TYPE AND DATES COVERED
	March 1995	Final report

4. TITLE AND SUBTITLE
Imaging Smolt Behavior on an Extended-Length Submerged Bar Screen and an Extended-Length Submerged Traveling Screen at The Dalles Dam in 1993

5. FUNDING NUMBERS

6. AUTHOR(S)
John Nestler, Robert Davidson

7. PERFORMING ORGANIZATION NAME(S) AND ADDRESS(ES)
U.S. Army Engineer Waterways Experiment Station
3909 Halls Ferry Road
Vicksburg, MS 39180-6199

8. PERFORMING ORGANIZATION REPORT NUMBER

9. SPONSORING/MONITORING AGENCY NAME(S) AND ADDRESS(ES)
U.S. Army Engineer District, Portland
P.O. Box 2946
Portland, OR 97208-2946

10. SPONSORING/MONITORING AGENCY REPORT NUMBER
Technical Report
EL-95-13

11. SUPPLEMENTARY NOTES
Available from National Technical Information Service, 5285 Port Royal Road, Springfield, VA 22161.

12a. DISTRIBUTION/AVAILABILITY STATEMENT
Approved for public release; distribution is unlimited.

12b. DISTRIBUTION CODE

13. ABSTRACT *(Maximum 200 words)*

The U.S. Army Engineer District, Portland, commissioned the Environmental and Hydraulics Laboratories, U.S. Army Engineer Waterways Experiment Station (WES), to conduct a study to facilitate the design and operation of fish bypass systems. A comparison of impingement behavior of smolts on extended-length submerged traveling screens and bar screens using underwater video imaging was made at The Dalles Dam. Smolt bypass systems were video imaged using low-light sensitive underwater cameras. These cameras recorded smolt behavior to two porosities and three discharges. Screen design had a significant effect on a number of impingement behavior variables and the standard deviation of water approach angles. The general observation was that the smolts can detect and more successfully avoid the traveling screens, while they are less able to detect the bar screens and are more likely to be imaged on or contacted by the bar screens.

The necessary monitoring equipment does not exist, but research and development of such systems is ongoing at WES as a part of this study.

14. SUBJECT TERMS			15. NUMBER OF PAGES
Bar screens	Fish passage	The Dalles	60
Bypass systems	Fish protection	Traveling screens	16. PRICE CODE
Fish impingement	Smolts	Video imaging	

17. SECURITY CLASSIFICATION OF REPORT	18. SECURITY CLASSIFICATION OF THIS PAGE	19. SECURITY CLASSIFICATION OF ABSTRACT	20. LIMITATION OF ABSTRACT
UNCLASSIFIED	UNCLASSIFIED		